An Observational Examination of Long-Lived Supercells. Part II: Environmental Conditions and Forecasting

MATTHEW J. BUNKERS, JEFFREY S. JOHNSON, AND LEE J. CZEPYHA
NOAA/National Weather Service, Rapid City, South Dakota

JASON M. GRZYWACZ
NOAA/National Weather Service, Dodge City, Kansas

BRIAN A. KLIMOWSKI
NOAA/National Weather Service, Bellemont, Arizona

MARK R. HJELMFELT
South Dakota School of Mines and Technology, Rapid City, South Dakota

(Manuscript received 26 August 2005, in final form 15 January 2006)

ABSTRACT

The local and larger-scale environments of 184 long-lived supercell events (containing one or more supercells with lifetimes ≥4 h; see Part I of this paper) are investigated and subsequently compared with those from 137 moderate-lived events (average supercell lifetime 2–4 h) and 119 short-lived events (average supercell lifetime ≤2 h) to better anticipate supercell longevity in the operational setting. Consistent with many previous studies, long-lived supercells occur in environments with much stronger 0–8-km bulk wind shear than what is observed for short-lived supercells; this strong shear leads to significant storm-relative winds in the mid- to upper levels for the longest-lived supercells. Additionally, the bulk Richardson number falls into a relatively narrow range for the longest-lived supercells—ranging mostly from 5 to 45. The mesoscale to synoptic-scale environment can also predispose a supercell to be long or short lived, somewhat independent of the local environment. For example, long-lived supercells may occur when supercells travel within a broad warm sector or else in close proximity to mesoscale or larger-scale boundaries (e.g., along or near a warm front, an old outflow boundary, or a moisture/buoyancy axis), even if the deep-layer shear is suboptimal. By way of contrast, strong atmospheric forcing can result in linear convection (and thus shorter-lived supercells) in a strongly sheared environment that would otherwise favor discrete, long-lived supercells.

1. Introduction

In Bunkers et al. (2006, hereafter Part I) it was shown that long-lived supercells (defined as supercells persisting for ≥4 h) are considerably more isolated[1] and discrete than short-lived supercells (defined as supercells with a lifetime ≤2 h), and they also produce notably more F2–F5 tornadoes than do short-lived supercells. Several regional variations in the long-lived supercell properties were documented across the United States, most prominently between the north-central United States (NCNTRL) and the Southeast. Because these longest-lived supercells present an operational forecasting concern and challenge—as well as a significant weather hazard to society—attention is now turned to the environmental conditions attending these supercell environments. Through this process, the goal is to gain a better awareness of the supercell longevity spectrum, especially with respect to operational forecasting applications.

a. Previous research on long-lived supercell environments

The fact that supercells are longer lived than nonsupercell thunderstorms derives from both a supercell's

[1] A supercell was considered isolated if it was separated from nearby cells by at least one storm diameter for >75% of its lifetime. This diameter was taken as the average diameter of the 35-dB*Z* echo. Furthermore, the convective mode of each long- and short-lived supercell event was classified as linear, discrete, or mixed (according to a supercell's relationship to linear convective features). Refer to Part I for more specific information regarding these definitions.

Corresponding author address: Dr. Matthew J. Bunkers, National Weather Service, 300 E. Signal Dr., Rapid City, SD 57701.
E-mail: matthew.bunkers@noaa.gov

persistent rotating updraft, which enhances vertical motion, as well as an *updraft–downdraft configuration*, which generally prevents precipitation from falling through the updraft (Marwitz 1972; Browning 1977; Lemon 1980; Weisman and Klemp 1986)—both of which, in turn, are dependent on the vertical wind shear. Indeed, several observational studies have shown a positive relationship between vertical wind shear and supercell occurrence (e.g., Chisholm and Renick 1972; Marwitz 1972; Fankhauser and Mohr 1977).

Corresponding to the above-mentioned observational studies, a plethora of numerical storm modeling studies has shown a similar relationship between vertical wind shear and supercell occurrence and longevity (e.g., Wilhelmson and Klemp 1978; Weisman and Klemp 1982; Droegemeier et al. 1993; Brooks et al. 1994a,b). Even though these studies have made it clear that supercell occurrence and persistence become more probable when the deep-layer vertical wind shear is strong (in the presence of conditional instability), they have not addressed quantitatively the relationship between supercell lifetime and vertical wind shear (or other parameters).

Storm-relative helicity (SRH) has been theorized to suppress turbulent dissipation, thus enabling supercell updrafts to be stable and long lived (Lilly 1986; Droegemeier et al. 1993). Because SRH is positively correlated with vertical wind shear, this theoretical claim is consistent with the observational and modeling results discussed above. However, SRH is almost always calculated in the lower atmosphere (over a layer $\leq$3 km AGL), and its importance to supercell longevity, relative to the vertical wind shear in the mid- and upper levels of the atmosphere, is not well understood. Nevertheless, observational studies have shown that SRH, on average, is larger in supercell environments than in nonsupercell environments (e.g., Rasmussen and Blanchard 1998; Thompson et al. 2003).

In addition to vertical wind shear, the lifted condensation level (LCL), and to a lesser extent the level of free convection (LFC), may also affect supercell longevity (McCaul and Cohen 2002). Through a combination of numerical modeling studies, McCaul and Cohen discussed that as the LCL height increased, stronger surface cold pools were produced, and thus multicells or squall lines tended to result instead of supercells (or else supercells experienced a premature[2] demise). Conversely, supercells tended to exhibit greater longevity when their downdraft strength and associated surface cold pools were minimized, as was the case in simulations with low-LCL–intermediate-LFC environments. Most observational documentation of LCL heights in supercell environments has pertained to tornadic versus nontornadic supercells (e.g., Rasmussen and Blanchard 1998; Markowski et al. 2002), and not to short- versus long-lived supercells.

In another numerical modeling study, Gilmore and Wicker (1998) showed that environmental relative humidity in the midtroposphere can have a significant impact on supercell evolution and longevity via modulation of the low-level outflow. For simulations with a relatively dry midtroposphere they found that evaporatively cooled downdrafts led to outflow that surged ahead of the storm (cutting off inflow), eventually causing the updraft and storm circulation to weaken prematurely. However, when the vertical wind shear was increased or the dry air was placed at a higher altitude, the outflow was not as strong and thus the supercell persisted for a longer period of time. Although McCaul and Cohen (2002) and Gilmore and Wicker (1998) discussed somewhat separate topics, they both addressed the critical role of evaporatively driven downdrafts in modulating the strength of the surface cold pool, which subsequently affects supercell evolution and longevity.

In addition to these near-storm environmental considerations, synoptic- and subsynoptic-scale features can also act to either enhance or limit the lifetime of a supercell. For example, Maddox et al. (1980) observed that tornadic storms crossing a thermal boundary tend to be shorter lived than tornadic storms moving parallel to a thermal boundary. Atkins et al. (1999) found modeled supercells were strongest and longest lived when they traveled along[3] preexisting boundaries or else toward the warm side, in contrast to storms initialized in a homogeneous environment or storms that traversed a boundary toward the cold side. Furthermore, they suggested storm motion, relative to boundary orientation, plays a key role in supercell evolution. Finally, Wilson and Megenhardt (1997) noted that storms moving in a direction opposite to a boundary layer convergence line (i.e., toward the cool side of the boundary) are unlikely

[2] The meaning of "premature" in this context is used to convey the idea that supercells will live longer if these detrimental influences are not present; this usage applies throughout the remainder of this paper. Clearly, it is very difficult to ascertain how much longer a supercell *might* live in the absence of these detrimental conditions—a problem also akin to understanding tornadic versus nontornadic environments [e.g., see discussion by Doswell et al. (2002, p. 938)].

[3] The meaning of "along" in this context does not necessarily suggest storms moved exactly along a boundary. It can also be taken to mean that a storm paralleled a boundary for most of its lifetime, but may have been within only 10s of kilometers of the boundary. This usage of along with respect to supercell motion applies throughout the remainder of this paper.

to persist, but storms with a velocity that nearly matches that of a boundary can persist for a relatively long duration.

Additional large-scale controls on supercell longevity include the strength and velocity of the forcing mechanisms as well as the orientation of forcing mechanisms relative to the vertical wind shear and mean wind (e.g., LaDue 1998; Bluestein and Weisman 2000; Roebber et al. 2002), which ultimately relates to the convective mode (Dial and Racy 2004). In a numerical simulation of the 3 May 1999 tornado outbreak, Roebber et al. (2002) found weak-to-moderate forcing favored the production of discrete long-lived supercells, but strong forcing resulted in a trend toward linear mesoscale convective systems (MCSs) in an environment with weak convective inhibition. Bluestein and Weisman (2000) modeled convection with different orientations of the vertical wind shear with respect to the line of forcing (e.g., cold fronts, drylines, etc.), and found this relationship can exert a significant influence on whether relatively isolated long-lived supercells develop or a squall line results. When the shear vector is aligned with a surface forcing mechanism, linear convection becomes likely (Dial and Racy 2004).

b. The present study

Although the above review provides some general guidance on the environments of long-lived supercells, much of it was based on numerical simulations rather than observations, and thus a thorough observational study that can be applied in the operational forecasting arena does not exist. Several important questions were also raised in Part I that cannot be answered based on previous research, especially with respect to the regional differences in long-lived supercell properties. Moreover, supercell motion and longevity may be interconnected, and this has yet to be thoroughly explored. In light of this, the present study takes the convective forecasting process described by McNulty (1995) one step further by asking the following: If supercells develop, will any be long lived, and what will the expected supercell lifetime be?

The overarching goal of this work is to develop an improved understanding of the relationships among 1) supercell lifetime, 2) supercell motion, and 3) the local and larger-scale environment, with a specific emphasis on helping the operational forecaster better anticipate supercell lifetime on any given day. It is hypothesized that supercell motion, which can be reasonably predicted when based on shear-relative techniques (Bunkers et al. 2000; Zeitler and Bunkers 2005), plays a key role in modulating supercell longevity (e.g., see Klimowski and Bunkers 2002, p. 1117). A consequence of this is that a supercell traveling with a similar velocity as a surface boundary or midlevel trough[4] may live longer than a supercell traveling differently than these features.

To accomplish the goal set forth above, the environments of 184 long-lived (LL; at least one supercell with a lifetime $\geq$ 4 h), 137 moderate-lived (ML; average supercell lifetime 2–4 h), and 113 short-lived (SL; average supercell lifetime $\leq$ 2 h) supercell events are examined; the definitions and acquisition of these supercell events were detailed in Part I. After describing the data and methods (section 2), results pertaining to the environments of the supercell events, including geographical variations across the United States, are discussed in section 3. In section 4 the implications of these results are summarized, and a conceptual model for forecasting long-lived supercells is presented.

2. Data and methods

Observed sounding information was collected, if possible, for each of the long-, moderate-, and short-lived supercell events from Part I. The following two criteria were required for at least 1 h of each event: (i) supercells occurred within 185 km (100 n mi) of the corresponding sounding location and (ii) supercells occurred within 3 h of the sounding valid time. Each observed sounding was screened for "representativeness" of the air mass in which the supercells occurred. This usually meant the sounding was valid for locations in the likely inflow region of a supercell, and was not contaminated by outflow from nearby thunderstorms, which would change the thermodynamic and kinematic structure of the boundary layer. These criteria are in general agreement with other observational studies (e.g., Brooks et al. 1994a; Rasmussen and Blanchard 1998; Bunkers et al. 2000; Evans and Doswell 2001).

In some cases a supercell event occurred in between two or more candidate sounding locations. Therefore, the sounding parameters (described below) were calculated for each of the sounding sites and then interpolated for the given event. This occurred for 12%–18% of all events (Table 1). Moreover, because of the incompleteness or unavailability of these observed soundings at times (e.g., the supercells were not close in time/space to a sounding site, or the low levels of a

[4] Note that the scale of vertical motion associated with a surface boundary (approximately 10 cm s^{-1}–1 m s^{-1}) is far different than that associated with a midlevel trough (approximately 1–10 cm s^{-1}). As such, the relatively small values associated with a midlevel trough make it insufficient to initiate deep moist convection; rather, it serves to condition the background environment (Doswell 1987).

TABLE 1. Sounding sources for the LL, ML, and SL supercell events. The total number of supercell events with sounding data for each classification is indicated in parentheses in the leftmost column. Under each column heading in the first row, the first (second) value indicates the number (percentage) of soundings for the corresponding classification. The radiosonde (raob) and RUC sources contain both thermodynamic and kinematic information; the NPN and WSR-88D sources contain kinematic information only.

	Single raob	Multiple raob	Single NPN	0-h RUC	Raob/WSR-88D/surface
LL (174)	115 (66.1%)	32 (18.4%)	6 (3.4%)	12 (6.9%)	9 (5.2%)
ML (137)	102 (74.4%)	16 (11.7%)	9 (6.6%)	8 (5.8%)	2 (1.5%)
SL (119)	87 (73.1%)	14 (11.8%)	9 (7.5%)	4 (3.4%)	5 (4.2%)

sounding were convectively contaminated), there were some occasions when the following data were utilized, based on availability: (i) Rapid Update Cycle (RUC) model analysis soundings (Thompson et al. 2003; Benjamin et al. 2004), (ii) National Oceanic and Atmospheric Administration (NOAA) Profiler Network (NPN) wind profiles, or (iii) surface data and Weather Surveillance Radar-1988 Doppler (WSR-88D) wind profiles for the boundary layer, with observed soundings above the boundary layer (Table 1). However, the majority (66%–74%) of the soundings consisted of single unmodified observations from the NOAA radiosonde network, and most (84%–86%) consisted only of radiosonde observations. Note that only kinematic profiles can be derived from the NPN data source, so small percentages (3%–8%) of the supercell events do not have any concurrent thermodynamic profiles (Table 1).

The mean-layer (ML) parcel in the lowest 1000 m and the virtual temperature correction (Doswell and Rasmussen 1994) were used to calculate sounding thermodynamic parameters. The ML parcel is believed to be more robust than the surface-based parcel (Bunkers et al. 2002; Craven et al. 2002) and is consistent with numerical modeling studies (e.g., Weisman and Klemp 1982). Calculated parameters included ML convective available potential energy (MLCAPE), ML convective inhibition (MLCIN), ML bulk Richardson number (MLBRN; Weisman and Klemp 1982), ML lifted condensation level (MLLCL), ML level of free convection (MLLFC), precipitable water from the surface to 300 hPa (PWAT), mean relative humidity from the surface to 700 hPa (RH7), mean relative humidity from 700 to 300 hPa (RH3), bulk and total wind shear for three different layers ($\text{Bulk}_{x-y\text{km}}$ and $\text{Total}_{x-y\text{km}}$: 0–4, 0–8, and 4–8 km), bulk Richardson number shear (BRNSHR), SRH for two different layers ($\text{SRH}_{x-y\text{km}}$: 0–1 and 0–3 km), and storm-relative winds for five different layers or levels ($\text{SRW}_{x-y\text{km}}$: 0–1, 0–3, 5, 8, and 7–10 km). The storm-relative winds were averaged over the respective layers at 500-m intervals, and observed supercell motions were used to calculate all storm-relative parameters.

A second environmental consideration for the long- and short-lived supercell events was the strength of the synoptic-scale forcing. This was evaluated in a manner similar to that done by Evans and Doswell (2001, p. 331; see their Fig. 1). A qualitative approach categorized these events into (i) strong forcing (SF), (ii) medium forcing (MF), or (iii) weak forcing (WF). The amplitude and/or strength of midlevel short-wave troughs, 300-hPa jets, and surface frontal systems carried the most weight in this taxonomy. Generally speaking, the SF events exhibited large-amplitude midlevel short-wave troughs, 300-hPa isotach maxima of >36 m s^{-1} (70 kt), and/or surface frontal boundaries with horizontal temperature gradients >5°C (100 km)$^{-1}$. The WF events were just the opposite, with 300-hPa isotach maxima generally <26 m s^{-1} (50 kt) and surface horizontal temperature gradients <2.5°C (100 km)$^{-1}$. This task was accomplished by consulting surface maps at 3-h intervals, mandatory-level pressure charts at 1200 and 0000 UTC, and Geostationary Operational Environmental Satellite imagery when available (mostly the 6.7-μm channel). Exceptions to the above guidelines included the following: (i) for cases with a strong baroclinic zone in the lower troposphere, but only a weak trough in the midlevels, the event was categorized as SF; and (ii) for cases with a 300-hPa isotach maximum of 26–36 m s^{-1} (50–70 kt), but no amplification to the midlevel flow and weak surface to lower-tropospheric features, the event was categorized as WF. Although this is a subjective procedure, any biases present in the dataset should be consistent between the long- and short-lived events, and therefore a relative comparison between the two supercell classifications is still expected to yield useful information.

As noted in section 1b, it is hypothesized that supercell motion and longevity are intertwined. Therefore, mesoscale to synoptic-scale data (i.e., surface, satellite, radar, and upper air) were used to characterize the motion of the long-lived supercells with respect to surface boundaries (e.g., fronts, outflow boundaries, and drylines), moisture/buoyancy axes, broad air masses, and mid- to upper-level forcing mechanisms [similar to Maddox et al. (1980)]. Subsequently, each *long-lived supercell* was grouped into one of six different categories based on this procedure:

1) Along: Supercell motion was either along a boundary (see footnote 3) or within 15° of a moisture/buoyancy axis, or at a similar velocity as a mid- to upper-level forcing mechanism.
2) Warm sector: The supercell remained within a broad, warm, and buoyant region.
3) Toward more buoyant: Supercell motion was at an angle (15°–90°) to a boundary or moisture/buoyancy axis, which directed the supercell toward increasingly moist/buoyant air.
4) Toward less buoyant: Supercell motion was at an angle (15°–60°) to a boundary or moisture/buoyancy axis, which directed the supercell toward increasingly dry/less buoyant air.
5) Quickly less buoyant: Supercell motion was at a large angle (>60°) to a boundary or moisture/buoyancy axis, which "quickly" directed the supercell toward increasingly dry/less buoyant air. There was no accounting for speed in differentiating between categories 4 and 5.
6) Cold/Overtaken: The supercell either remained in the cold sector of an extratropical cyclone, or else it was overtaken by a frontal boundary, prefrontal squall line, or mid- to upper-level forcing mechanism.

The first three categories are considered to be favorable for continued supercell survival, whereas the last three categories are believed to potentially limit supercell lifetime.

3. Results and discussion

a. Environments of the supercell events

1) SOUNDING PARAMETERS

A correlation matrix was constructed for the 22 parameters outlined in section 2, using the sounding data for the long-lived supercell events (Table 2). Overall, RH3 has the weakest correlation coefficients—and thus the greatest degree of independence—among all of the parameters, with the strongest value of −0.21 associated with MLCAPE. PWAT has low correlation coefficients as well; the largest value is only 0.47 in relation to RH7. On the other hand, several of the shear parameters have rather large values, indicating substantial interdependence. For example, the correlation coefficient between $\text{Bulk}_{0\text{–}4\text{km}}$ and BRNSHR is 0.84, with their coefficients in relation to the other parameters nearly approximating one another. After review of the correlation matrix, 14 parameters were considered for further investigation based on their relative degrees of independence: $\text{Total}_{0\text{–}8\text{km}}$, $\text{Bulk}_{0\text{–}8\text{km}}$, BRNSHR, $\text{SRH}_{0\text{–}3\text{km}}$, $\text{SRW}_{0\text{–}3\text{km}}$, $\text{SRW}_{5\text{km}}$, $\text{SRW}_{8\text{km}}$, MLCAPE, MLCIN, MLBRN, MLLCL, MLLFC, PWAT, and RH3.

Use of box-and-whisker plots (Wilks 1995) helped further reduce the parameters from 14 to 8 (Fig. 1), based in part on the least interquartile overlap across categories of supercellular lifespan. Several of these parameters revealed a gradual shift in the distributions across the supercell longevity spectrum, but $\text{Bulk}_{0\text{–}8\text{km}}$ displayed the largest and most significant differences with no overlap of the interquartile ranges for the three supercell classifications (Fig. 1, top left-hand plot; Table 3a). This agrees well with the previous observational and modeling studies outlined in section 1a, and furthermore, it helps quantify the heretofore nebulous relationship between supercell longevity and deep-layer shear; as $\text{Bulk}_{0\text{–}8\text{km}}$ strengthens above 26 m s^{-1} (50 kt), long-lived supercells become increasingly likely. The BRNSHR plot resembles that of $\text{Bulk}_{0\text{–}8\text{km}}$, but there is more overlap in the distributions for BRNSHR (Fig. 1) and, thus, smaller Student's t test statistics (Table 3a). Note that the more traditional $\text{Bulk}_{0\text{–}6\text{km}}$ and $\text{Bulk}_{0\text{–}3\text{km}}$ were also tested, but the results were inferior to $\text{Bulk}_{0\text{–}8\text{km}}$ (Table 3), with an overlap in the box-and-whisker plots (not shown) similar to that for BRNSHR. These results make it apparent that a deeper measure of the vertical wind shear (i.e., >0–6 km) is most appropriate when evaluating the potential for long-lived supercells, which is consistent with the findings of Thompson et al. (2004).

Another relatively strong signal is evident in the $\text{SRW}_{8\text{km}}$ distribution (Fig. 1, top right-hand plot), with $\text{SRW}_{8\text{km}}$ >17 m s^{-1} (33 kt) for 75% of the long-lived supercell events, and <16 m s^{-1} (31 kt) for 75% of the short-lived supercell events. This is consistent with the results for $\text{Bulk}_{0\text{–}8\text{km}}$, albeit the signal is not as strong (Table 3a). Rasmussen and Straka (1998) found the upper-level storm-relative flow was weakest, on average, in the environments of high-precipitation supercells. A scatterplot of $\text{Bulk}_{0\text{–}8\text{km}}$ versus $\text{SRW}_{8\text{km}}$ (Fig. 2) reveals the propensity for long-lived supercell events to occur with increasing values of each parameter (recall $r = 0.76$ between the two variables; Table 2).

The MLBRN (i.e., MLCAPE/BRNSHR) shows limited potential for forecasting supercell longevity, with progressively smaller values favoring long-lived supercell events (Fig. 1). The range of MLBRN for long-lived supercell events is rather narrow, 6–36 for the inner 80% of the distribution, and 5–46 for the inner 90%, which is in very good agreement with the seminal work by Weisman and Klemp (1982) as well as the ensemble cloud modeling study by Elmore et al. (2002; see their Fig. 13). Despite the statistically significant difference

TABLE 2. Correlation matrix for the 22 sounding parameters evaluated for the long-lived supercell events in the present study. The digits across the top row correspond to the numbered fields on the side. Correlation coefficients r with an absolute value > 0.13 (0.17) are significantly different from zero at the $\alpha = 0.05$ (=0.01) level. Data were available for 174 of the 184 events. See section 2 for a definition of the parameters.

	1	2	3	4	5	6	7	8	9	10	11	12	13	14	15	16	17	18	19	20	21	22
1) $Total_{0–4km}$	1.0																					
2) $Total_{4–8km}$	0.16	1.0																				
3) $Total_{0–8km}$	0.76	0.76	1.0																			
4) $Bulk_{0–4km}$	0.60	−0.06	0.36	1.0																		
5) $Bulk_{4–8km}$	−0.11	0.74	0.42	−0.28	1.0																	
6) $Bulk_{0–8km}$	0.30	0.60	0.59	0.41	0.70	1.0																
7) BRNSHR	0.67	0.05	0.47	0.84	−0.11	0.47	1.0															
8) $SRH_{0–1km}$	0.71	0.22	0.61	0.37	0.05	0.27	0.57	1.0														
9) $SRH_{0–3km}$	0.70	0.13	0.55	0.44	−0.02	0.25	0.64	0.80	1.0													
10) $SRW_{0–1km}$	0.45	0.08	0.35	0.41	0.07	0.37	0.52	0.30	0.59	1.0												
11) $SRW_{0–3km}$	0.26	0.13	0.26	0.18	0.17	0.30	0.22	0.19	0.54	0.88	1.0											
12) SRW_{5km}	0.18	0.17	0.23	0.44	0.06	0.32	0.35	−0.06	0.06	0.03	0.03	1.0										
13) SRW_{8km}	−0.02	0.59	0.38	−0.01	0.76	0.76	0.02	−0.09	−0.11	−0.01	0.04	0.40	1.0									
14) $SRW_{7–10km}$	−0.06	0.57	0.34	−0.03	0.72	0.70	−0.02	−0.12	−0.14	−0.02	0.04	0.40	0.93	1.0								
15) MLCAPE	−0.06	−0.08	−0.10	−0.01	−0.08	−0.14	−0.02	0.02	0.03	0.01	0.00	0.00	−0.06	−0.07	1.0							
16) MLCIN	−0.03	−0.01	−0.02	0.08	−0.03	0.01	−0.01	−0.03	−0.06	−0.18	−0.15	0.13	0.03	0.03	0.18	1.0						
17) MLBRN	−0.40	−0.07	−0.31	−0.50	0.03	−0.34	−0.54	−0.27	−0.29	−0.25	−0.07	−0.18	−0.01	−0.01	0.74	0.14	1.0					
18) MLLCL	−0.23	−0.14	−0.25	−0.11	−0.04	−0.07	−0.23	−0.33	−0.15	0.11	0.17	−0.05	0.06	0.03	−0.03	−0.08	0.07	1.0				
19) MLLFC	−0.12	−0.07	−0.13	−0.26	−0.02	−0.14	−0.22	−0.13	−0.01	0.18	0.23	−0.31	−0.09	−0.07	−0.23	0.59	−0.09	0.40	1.0			
20) PWAT	0.18	0.04	0.15	0.02	−0.04	−0.10	0.07	0.29	0.18	0.10	0.08	−0.13	−0.21	−0.21	0.30	0.18	0.18	−0.35	−0.23	1.0		
21) RH7	0.22	0.08	0.20	0.11	0.01	0.03	0.19	0.28	0.15	−0.06	−0.12	0.04	−0.11	−0.08	−0.07	−0.39	−0.13	−0.74	−0.45	0.47	1.0	
22) RH3	0.01	−0.07	−0.04	0.08	−0.10	−0.03	0.01	0.00	−0.03	0.13	0.13	0.06	−0.09	−0.12	−0.21	0.00	−0.13	0.19	0.05	0.16	0.00	1.0

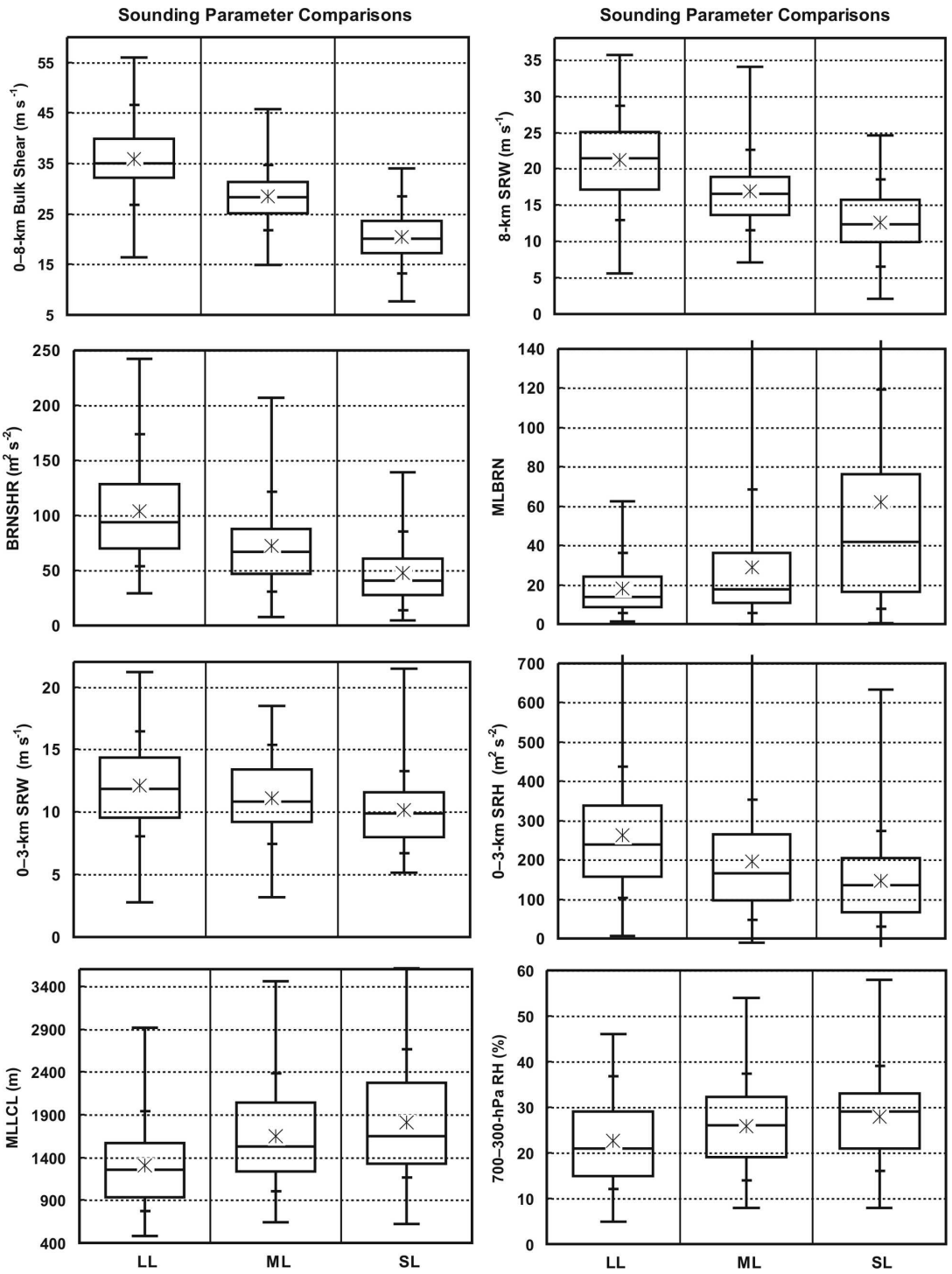

FIG. 1. Box-and-whisker plots (Wilks 1995) for the LL, ML, and SL supercell events using the sounding database and parameters described in section 2. For each individual plot, the middle 50% of the distribution is contained within the box, the horizontal line in the middle of the box represents the median value, the asterisk represents the mean value, the short horizontal dash on the upper (lower) whisker represents the 90th (10th) percentile, and the top (bottom) of the whisker represents the maximum (minimum) value. In a few cases the maximum/minimum values are truncated for display purposes.

TABLE 3. (a) Student's t test statistics for differences in means based on the eight parameters given in Fig. 1 for the various combinations of LL, ML, and SL supercell events. (b) Same as (a) but for ancillary parameters of interest not included in Fig. 1. Absolute values > 1.65 (>2.34) indicate significance at the $\alpha = 0.05$ ($=0.01$) level. See section 2 for a definition of the parameters.

	(a)		
	LL/SL	LL/ML	ML/SL
$Bulk_{0–8km}$	20.47	10.26	11.51
SRW_{8km}	13.20	6.76	7.37
BRNSHR	11.91	6.61	5.76
MLBRN	−7.45	−4.14	−4.52
$SRW_{0–3km}$	5.07	2.77	2.51
$SRH_{0–3km}$	7.11	3.93	2.94
MLLCL	−7.63	−5.62	−2.10
RH3	−4.63	−3.00	−1.72
	(b)		
$Bulk_{0–6km}$	15.01	7.93	7.64
$Bulk_{0–3km}$	10.43	5.06	5.25
$Bulk_{0–1km}$	5.68	4.89	0.80
$SRH_{0–1km}$	7.28	7.93	1.75

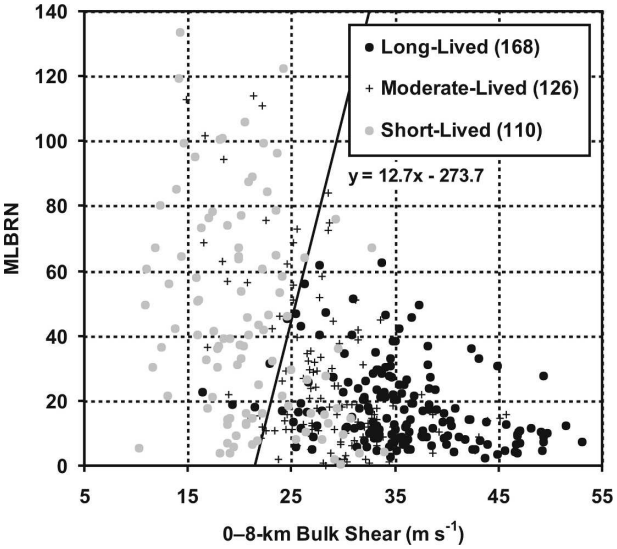

FIG. 3. Same as in Fig. 2 but for $Bulk_{0–8km}$ vs MLBRN. There are six (nine) fewer long-lived (short lived) cases in this figure than in Fig. 2 because of missing thermodynamic data.

in means (Table 3a), there is considerable overlap in the MLBRN distributions for all three supercell classifications with virtually no practical ability to distinguish between long- and moderate-lived supercell events. This is not surprising because MLBRN is more of a supercell versus multicell predictor than it is a long-lived versus shorter-lived supercell predictor. Nevertheless, MLBRN may be useful as a filter for long-lived supercell events (i.e., if the MLBRN is <5 or >45, long-lived supercells become unlikely), but it should not be used as a sole predictor. When MLBRN is viewed in conjunction with $Bulk_{0–8km}$ (Fig. 3), it appears that if MLBRN > 40, then $Bulk_{0–8km}$ must be relatively large for long-lived supercells to occur, and if MLBRN < 40, long-lived supercells can occur with relatively smaller $Bulk_{0–8km}$. This implies that deep-layer shear is not as critical to long-lived supercells when buoyancy is subpar. Finally, the short-lived supercell events corresponding exclusively to small MLBRN (≤ 5) environments were associated with very low MLCAPE (average of 233 J kg^{-1})—compared with 611 J kg^{-1} for the long-lived events with MLBRN ≤ 5. This suggests there was not enough buoyancy to sustain these short-lived supercells, which were in the presence of relatively strong wind shear.

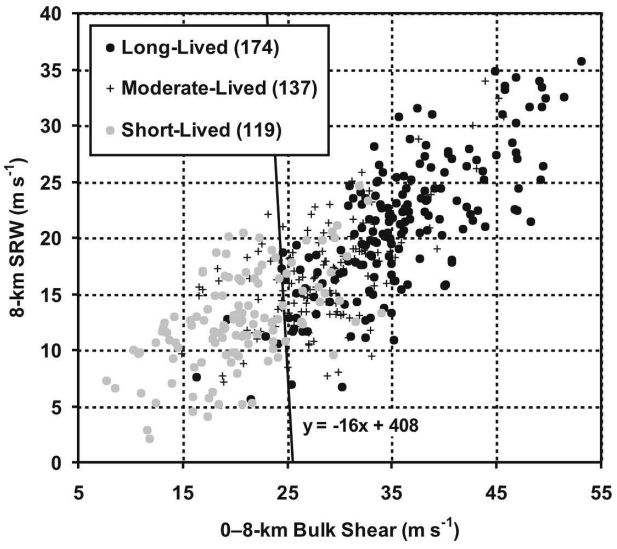

FIG. 2. Scatterplot of $Bulk_{0–8km}$ vs SRW_{8km} for the three supercell classifications in the present study. A line has been drawn to discriminate between the long- and short-lived supercell events so as to minimize the number of misclassified events, and the equation for the line is also given.

Most of the thermodynamic parameters were not as useful as the shear parameters in discriminating among the supercell classifications. The only one that appears reasonably effective is the MLLCL, which suggests long-lived supercell events are more probable as MLLCL heights, and hence cloud bases, decrease (Fig. 1, bottom left-hand plot; Table 3a). Generally speaking, the values of MLLCL range from 300 to 700 m lower for the long-lived supercell events when compared with the other two classifications. The scatterplot of $Bulk_{0–8km}$ versus MLLCL (Fig. 4) demonstrates the greatest ability to discriminate between long- and short-lived supercell events when compared with the other parameter

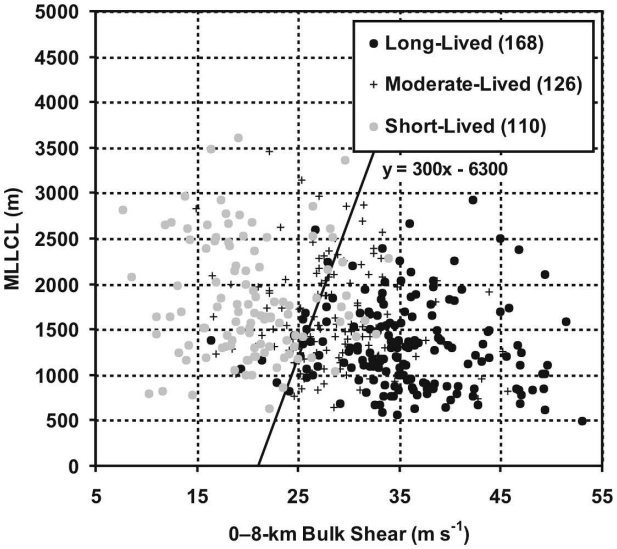

FIG. 4. Same as in Fig. 2 but for $\text{Bulk}_{0\text{–}8\text{km}}$ vs MLLCL. There are six (nine) fewer long-lived (short lived) cases in this figure than in Fig. 2 because of missing thermodynamic data.

combinations; this may be a result of $r = -0.07$ for $\text{Bulk}_{0\text{–}8\text{km}}$ and MLLCL, indicating the independence of the two variables. Indeed, only 10 long-lived events are left of the line in the plot, while 12 short-lived events fall to the right. It can be seen that $\text{Bulk}_{0\text{–}8\text{km}}$ may be suboptimal for long-lived events provided MLLCL heights are low. These findings are congruent with the numerical modeling results of McCaul and Cohen (2002; discussed in section 1a), and they also concur with the findings of Part I, Rasmussen and Blanchard (1998), and Thompson et al. (2003). Namely, long-lived supercells and significantly tornadic supercells are associated with lower MLLCL heights, on average, than are short-lived supercells and weakly tornadic or nontornadic supercells, respectively. Despite the benefits of viewing the MCLCL/$\text{Bulk}_{0\text{–}8\text{km}}$ parameter space, operational forecasters are cautioned against using this as a "cure-all" for forecasting supercell longevity.

Interestingly, RH3 displays a gradual decrease as one goes from short-lived to long-lived supercell events (Fig. 1, bottom right-hand plot), although the overlap among the three distributions is considerable. This may initially seem at odds with Gilmore and Wicker (1998), but recall that relatively large $\text{Bulk}_{0\text{–}8\text{km}}$ values correspond to this midtropospheric dryness for the long-lived events, which helps mitigate against strong low-level outflow, according to their study. Furthermore, the altitude of the RH3 layer aligns more closely with the "high altitude" dry air placement in Gilmore and Wicker (i.e., 3.5 instead of 2.3 km), which has less of an effect on the strength of a storm's low-level outflow when compared with dry air at lower levels. Be aware that the above results that are dependent on relative humidity (i.e., RH3, MLLCL, and to a lesser extent MLBRN) should be viewed with a bit of caution because of the approximate 5% dry bias in radiosonde relative humidity profiles (Turner et al. 2003), which can amount to a 0.5 g kg^{-1} dry bias in the mixing ratio throughout the boundary layer.

Given the widespread operational use of $\text{SRH}_{0\text{–}3\text{km}}$ as it pertains to severe local storms, and especially supercells, its efficacy with respect to supercell longevity was evaluated. In agreement with the modeling results of Droegemeier et al. (1993), average $\text{SRH}_{0\text{–}3\text{km}}$ was largest for the long-lived supercell events (Fig. 1), with just over 75% (50%) of the values >150 $\text{m}^2\,\text{s}^{-2}$ (225 $\text{m}^2\,\text{s}^{-2}$). Davies-Jones et al. (1990) proposed using 150 $\text{m}^2\,\text{s}^{-2}$ as a rough lower threshold for *mesocyclone* formation, which appears too high given the present results (assuming representativeness of kinematic sounding data to actual near-storm environments); 45% of the moderate-lived supercell events were associated with $\text{SRH}_{0\text{–}3\text{km}}$ below this value. Droegemeier et al. (1993) revised this general threshold upward to 250 $\text{m}^2\,\text{s}^{-2}$, which also is too high based on Fig. 1; over half of the long-lived supercell events had $\text{SRH}_{0\text{–}3\text{km}} < 250$ $\text{m}^2\,\text{s}^{-2}$. Therefore, given this information, plus the overlap in the $\text{SRH}_{0\text{–}3\text{km}}$ distributions, $\text{SRH}_{0\text{–}3\text{km}}$ clearly cannot be used alone as a discriminator of supercell longevity. For completeness, Student's t test statistics for differences of means were also computed for $\text{Bulk}_{0\text{–}3\text{km}}$ (Table 3b), and the results suggest $\text{SRH}_{0\text{–}3\text{km}}$ is slightly inferior to $\text{Bulk}_{0\text{–}3\text{km}}$ when discriminating among the supercell classes. Last, $\text{SRW}_{0\text{–}3\text{km}}$, an integral part of $\text{SRH}_{0\text{–}3\text{km}}$, was >7–8 m s^{-1} for 90% of all three of the supercell classifications (Fig. 1), which is in general support of the claim that this value should be at least 10 m s^{-1} for supercell storms (Droegemeier et al. 1993).

The relevance of $\text{Bulk}_{0\text{–}8\text{km}}$ versus $\text{SRH}_{0\text{–}3\text{km}}$ is quantified further by way of contingency tables. Statistics for the short- and moderate-lived supercell events were amalgamated, and then compared as a whole to the long-lived supercell events. The best discriminator between the long-lived and "other" supercell events was determined for both $\text{Bulk}_{0\text{–}8\text{km}}$ (i.e., 30 m s^{-1}) and $\text{SRH}_{0\text{–}3\text{km}}$ (i.e., 215 $\text{m}^2\,\text{s}^{-2}$), and then the probability of detection (POD), false alarm ratio (FAR), true skill score (TSS), and Heidke skill score (HSS) were calculated for each. The TSS approaches the POD when the forecast contingency table is dominated by correct nulls (Doswell et al. 1990), which is not true in the present study despite the large number of them; the HSS circumvents the null-dominance problem of the TSS and maintains most of its robustness. Expectedly, the POD

TABLE 4. Contingency tables for the LL supercell events vs the combination of ML and SL supercell events using (a) $Bulk_{0–8km}$ with 30 m s^{-1} as a discriminator and (b) $SRH_{0–3km}$ with 215 m^2 s^{-2} as a discriminator. Statistical measures were calculated as in Doswell et al. (1990). "Perfect" scores for the four measures are POD = 100%, FAR = 0%, TSS = 1.0, and HSS = 1.0.

(a)

		LL event observed		
		Yes	No	Tot
LL event forecast	Yes	147	53	200
	No	27	203	230
	Tot	174	256	430
	POD = 84%	FAR = 27%		
	TSS = 0.64	HSS = 0.62		

(b)

		LL event observed		
		Yes	No	Tot
LL event forecast	Yes	101	64	165
	No	73	192	265
	Tot	174	256	430
	POD = 58%	FAR = 39%		
	TSS = 0.33	HSS = 0.33		

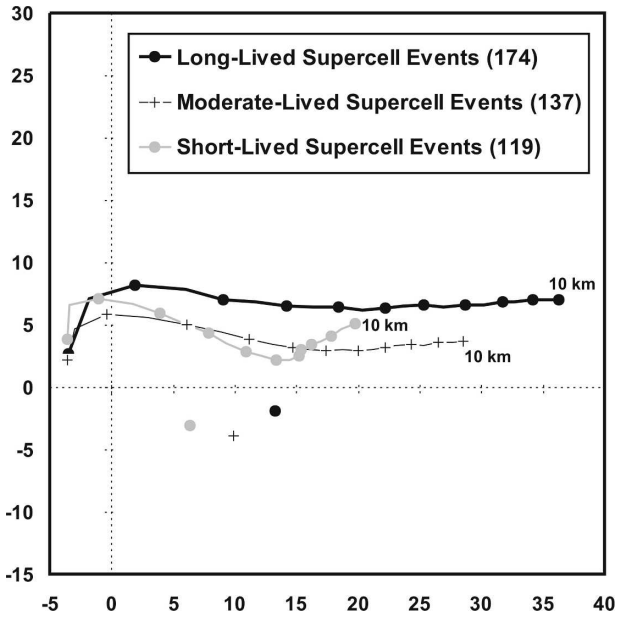

FIG. 5. Composite 0–10-km hodographs and observed storm motions (m s^{-1}) for the long-lived (solid circles), moderate-lived (plus signs), and short-lived (gray circles) supercell events. Prior to averaging, individual hodographs were translated such that the 0–0.5- to 5.5–6-km shear vector was positively aligned with the *x* axis, and the 0–0.5-km wind was at the origin. After averaging of the individual hodographs, the resulting composite hodographs were readjusted by adding back the composite mean wind and aligning with the composite 0–0.5- to 5.5–6-km shear vector (both obtained prior to the initial translation/averaging process) for each of the individual classifications. Data are plotted every 500 m, but markers are only given at 1-km intervals.

was 26% higher and the FAR was 12% lower for $Bulk_{0–8km}$ versus $SRH_{0–3km}$ when discriminating between the long-lived and other supercell events (Table 4). Moreover, the TSS and HSS for $Bulk_{0–8km}$ were both about double the values for $SRH_{0–3km}$ (unity indicates a perfect score). These results are in good agreement with Table 3.

A synthesis of the above results supports the idea that deep-layer shear and upper-level storm-relative winds are more appropriate than low-level shear/SRH when evaluating the potential for long-lived supercells (also see Weisman and Rotunno 2000). Even with large $SRH_{0–3km}$, if the storm-relative winds and shear are not strong enough in the mid- to upper levels, more precipitation falls near the updraft, potentially creating an intense downdraft and strong low-level outflow (Brooks et al. 1994b; Rasmussen and Straka 1998), thus shortening the supercell lifetime. For example, numerical modeling results (e.g., UCAR 2005; cf. their D2 and M2 simulations) provide evidence of longer-lived supercells in environments with greater $Bulk_{0–8km}$ and SRW_{8km}, but much less $SRH_{0–3km}$ (e.g., D2), than for simulations portraying shorter-lived supercells (e.g., M2). The importance of strong shear over a deep layer for long-lived supercell events is also evinced in the composite hodographs for the three classifications in the present study (Fig. 5). The long-lived composite hodograph curves by ~90° in the lowest 1 km and then displays strong unidirectional shear. Indeed, the 4–8-km bulk shear for the long-lived composite hodograph is nearly as strong as the 0–4-km bulk shear for the short-lived composite, reiterating the significance of mid- to upper-level shear.

Given the usefulness of $SRH_{0–1km}$ in distinguishing between significantly tornadic supercells and weakly tornadic or nontornadic supercells (Rasmussen 2003; Thompson et al. 2003), and also because of the apparent connection between supercell longevity and significant tornadoes (Part I), this parameter is investigated further here. Based on the box-and-whisker plots there is substantial overlap of the moderate- and short-lived distributions (Fig. 6), and the differences in the means are not significant at the $\alpha = 0.01$ level (Table 3b). However, the long-lived distribution for $SRH_{0–1km}$ is significantly different than both the moderate- and short-lived distributions (Fig. 6; Table 3b)—even more so than for $SRH_{0–3km}$ and $Bulk_{0–1km}$. Rasmussen and Blanchard (1998), Rasmussen (2003), and Thompson et al. (2003) found that $SRH_{0–1km}$ is highest and MLLCL is lowest, on average, in the environments of significantly tornadic supercells. Thus, the combination of

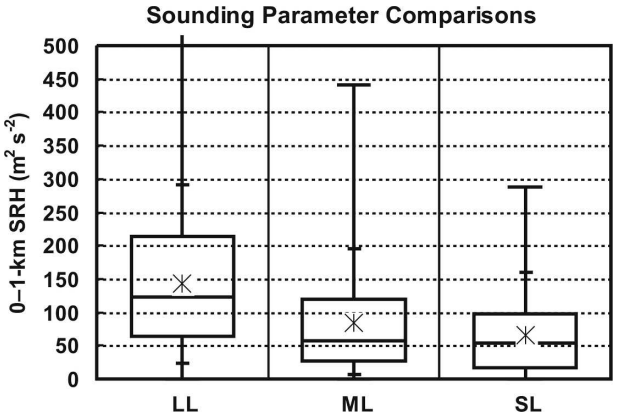

FIG. 6. Same as in Fig. 1 but for $SRH_{0–1km}$.

these previous studies with Part I and the present results for $SRH_{0–1km}$ and MLLCL suggests that environments of long-lived supercells appear to be more supportive of F2–F5 tornadoes when compared with those environments of moderate- and short-lived supercells.

2) THE MESOSCALE TO SYNOPTIC-SCALE ENVIRONMENT

Using the previously described stratification of WF, MF, and SF, a mild relationship is apparent between supercell lifetime and forcing strength (Table 5). Nearly half (49%) of the long-lived supercell events were associated with MF environments. And although about one-third (30%) of the long-lived events occurred in SF environments, the average lifetime of these supercells (5.0 h) is considerably less than for the MF cases (5.8 h). The lowest percentage of long-lived events occurred in WF environments (21%), but this is where most of the short-lived supercell events resided (57%). Therefore, there is a tendency for longer-lived supercells to occur with greater frequency as the environmental forcing strength increases from WF to MF. Considering the importance of deep-layer vertical wind shear to long-lived supercells (see the previous section) and given the correlation coefficient between $Bulk_{0–8km}$ and forcing strength equals 0.45, this result is intuitive.

A refined perspective emerges when the forcing strength categories are sorted by convective mode (Table 6). For the long-lived supercell events, the MF and WF categories were dominated by a discrete convective mode (76%–79%), with only about one-fifth for the mixed convective mode (18%–24%). When long-lived supercells occurred in SF environments, there was almost a split between the discrete and mixed modes. The lifetimes of the long-lived supercells were greatest in the MF environments when a discrete convective mode was displayed (5.9 h) and shortest in the SF environments with a linear convective mode (4.6 h), excluding the sole WF linear case (Table 6).

TABLE 5. Forcing strength for the LL and SL supercell events. The total number of supercell events with mesoscale to synoptic-scale data for each forcing classification is indicated in parentheses in the leftmost column. Below each column heading in the first row, the first value indicates the categorical forcing percentage for the corresponding event, and the second number represents the average lifetime of the long-lived supercells for each of the three forcing categories. The average lifetime for all long-lived supercells was 5.5 h.

	SF	MF	WF	Tot
LL (184)	30% (5.0 h)	49% (5.8 h)	21% (5.4 h)	100%
SL (119)	10%	33%	57%	100%

These results are corroborated by observations from the moderate-lived supercell events; at least 10 cases were observed in which SF environments were associated with upscale growth and/or the transition into a linear convective mode. In fact, the composite hodograph and sounding parameters from this subset of 10 moderate-lived events (not shown) aligns most closely with those for the long-lived supercell events (Fig. 5). Therefore, the mesoscale to synoptic-scale environment likely was a determining factor in the "premature demise" of these supercells from the 10 moderate-lived events. With respect to the short-lived supercell events, there is a clear tendency for linear-to-mixed convective modes in the SF environments and mixed-to-discrete convective modes in the WF environments (Table 6), suggesting that as forcing strength increases, so does the tendency toward linear organization. Recall that Roebber et al. (2002) found WF–MF environments favored the production of discrete long-lived supercells in the 3 May 1999 tornado outbreak, but their simulated SF resulted in a trend toward linear MCSs (and hence shorter-lived supercells).

The hodographs for the long-lived supercell events that occurred under both SF environmental conditions and displayed a linear convective mode were examined (seven total). The composite hodograph (Fig. 7) had even stronger bulk shear than what was present in Fig. 5 for all long-lived events, especially for $Bulk_{4–8km}$ (20.0 versus 13.3 m s^{-1}). This resulted in an SRW_{8km} that was 4.2 m s^{-1} stronger as well. The composite hodograph for the short-lived supercell events, given the same SF and linear convective mode constraints as above (three total; Fig. 7), also had stronger bulk shear than the composite for the short-lived events in Fig. 5, particularly in the low levels. Even though the 0–4-km bulk shear was 6.6 m s^{-1} stronger in the composite hodograph for this small subset (Fig. 7), the 4–8-km

TABLE 6. Forcing strength for the LL and SL supercell events sorted by convective mode. Percentages are given for each combination of convective mode and forcing strength, and the average lifetime of the long-lived supercells for each combination is also given. The total number of supercell events for the various classifications is indicated in parentheses. The average lifetime for all long-lived supercells was 5.5 h.

	Convective mode	SF (57)	MF (88)	WF (39)
LL (8)	Linear	13%/4.6 h (7)	—	3%/4.0 h (1)
LL (52)	Mixed	41%/4.9 h (23)	24%/5.7 h (22)	18%/5.9 h (7)
LL (124)	Discrete	46%/5.3 h (26)	76%/5.9 h (68)	79%/5.4 h (30)
Tot (184)		100%	100%	100%
		SF (12)	MF (39)	WF (66)
SL (15)	Linear	25% (3)	23% (9)	5% (3)
SL (59)	Mixed	67% (8)	49% (19)	48% (32)
SL (43)	Discrete	8% (1)	28% (11)	47% (31)
Tot (117)		100%	100%	100%

bulk shear was almost identical between this subset and the full short-lived composite, producing only a 1.8 m s^{-1} difference in SRW_{8km} (slightly stronger, on average, for these three cases). Once again, these results (although only based on a single-digit sample size) highlight the importance of the upper-level shear and storm-relative winds in supporting long-lived supercells, which appears progressively more critical when the forcing strength becomes strong and a linear convective mode is present.

Not only is the forcing *strength* germane to supercell longevity and the convective mode, but the *velocity* of various forcing mechanisms, with respect to supercell motion, can be just as important. In at least 14 (or 8%) of the 184 long-lived supercell events, supercells were either overtaken by forcing mechanisms of varying scale (i.e., fronts or short-wave troughs; note the caveat in footnote 4), or else they gradually fell behind in the cold sector of an extratropical cyclone. The average lifetime of these supercells was 4.4 h, which is significantly less than the 5.5-h average for all long-lived supercells (see Part I). Thus, it is plausible that these forcing mechanisms of varying scale (i) made the environments that the long-lived supercells were traveling through unfavorable and/or (ii) helped to organize and strengthen the outflow boundaries (or other mesoscale boundaries) such that the supercells grew upscale into MCSs. Indeed, it may be that the longest-lived supercells are a result of the storm maintaining a similar velocity as its attendant forcing mechanism (i.e., not outrunning the forcing and not being overtaken by it).

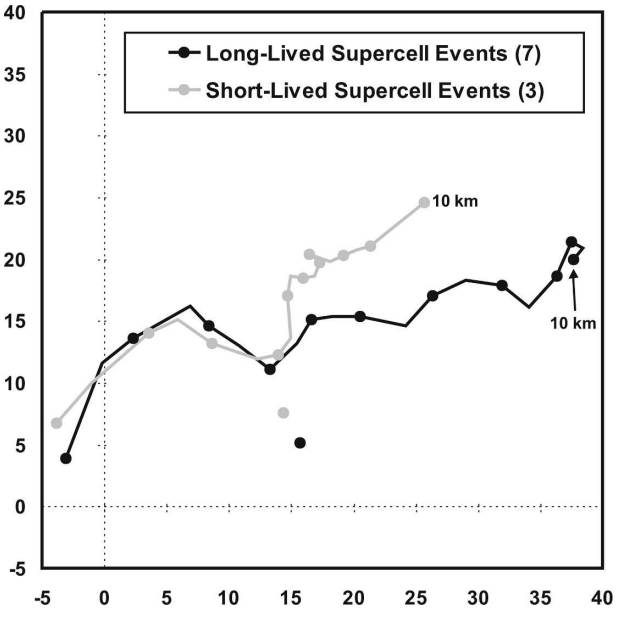

FIG. 7. Composite 0–10-km hodographs and observed storm motions (m s^{-1}) for the long-lived (solid circles) and short-lived (gray circles) supercell events that both occurred in SF environments and also displayed a linear convective mode. Otherwise the same as in Fig. 5.

The hypothesis that supercell motion is one determinant of supercell longevity was further tested as outlined in section 2. The most prominent finding from this evaluation is that just over half (51%) of all long-lived supercells had a significant component of their motion somewhat parallel to a boundary or moisture/buoyancy axis, or else at a similar speed as a mid- to upper-level forcing mechanism (Fig. 8). The average lifetime of these supercells was 5.9 h, or 0.4 h more than the average for the entire long-lived dataset. A much smaller fraction of long-lived supercells occurred in the warm sector away from discernable boundaries (18%), but these also had a correspondingly high average lifetime (6.0 h). The long-lived supercells with the greatest average lifetime (6.3 h) were the ones that gradually traveled toward increasingly moist/buoyant air. These supercells may have crossed a boundary, or they may have formed upstream of a moisture/buoyancy axis and then gradually moved toward it.

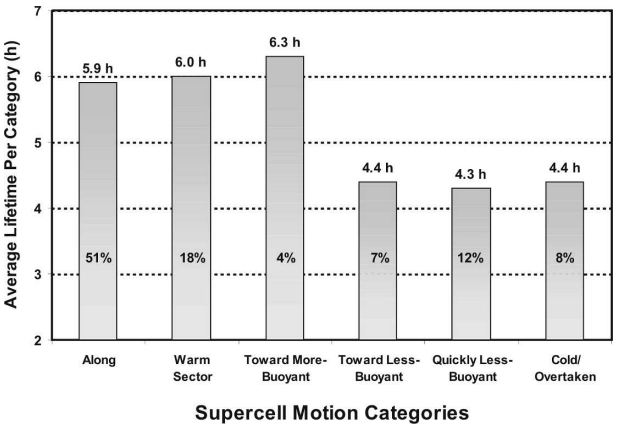

FIG. 8. Average lifetime of the long-lived supercells for each of the six supercell motion categories given in section 2. The percentage of cases (out of 180 total) for each category is also given inside the shaded vertical bars.

By contrast, long-lived supercells that moved toward increasingly dry/less buoyant air had a much shorter lifetime, on average, than the rest of the long-lived supercells (4.3–4.4 h; Fig. 8). This result did not seem to depend on what angle the supercells were traveling at with respect to the boundaries, although the sample size is too small to be certain of this. What is relevant, however, is that when the supercell motion was such that it took the storm away from a "favorable" environment into a "less favorable" environment, the average supercell lifetime was diminished. In fact, the average supercell lifetime for the three favorable categories was 6.0 h (Fig. 8, left-hand side), and the average supercell lifetime for the three "unfavorable" categories was 4.3 h (Fig. 8, right-hand side). This difference is statistically significant at $\alpha = 0.0001$ based on the Student's t test. Reinforcing these results is that the differences in the mean sounding parameters between the favorable and unfavorable categories were mostly $<5\%$–10%.

An intriguing question that arises from the above observations is: Does a boundary force a supercell to move along it, or does a supercell move along a boundary because of the coincidence of the supercell's shear-induced motion with the boundary? As alluded to above, there were several instances when supercells traveled at an angle to a boundary, crossed the boundary, and then weakened [also see Markowski et al. (1998) and Rasmussen et al. (2000)]. Furthermore, the observed supercell motion for the entire long-lived

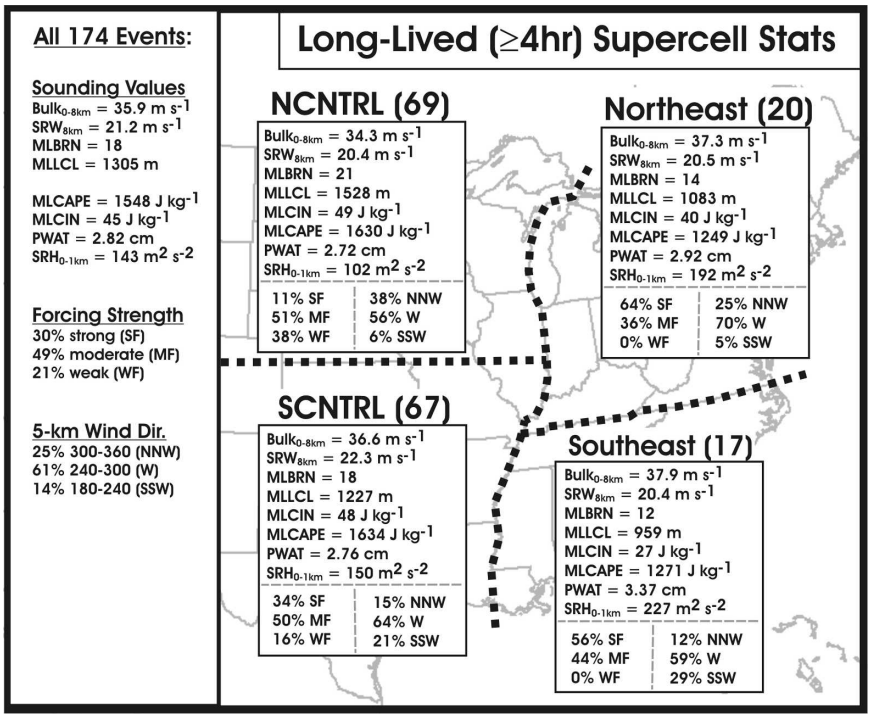

FIG. 9. (left) Average sounding parameters for 174 (out of the 184) long-lived supercell events, along with the same parameters for (right) each of four arbitrarily defined regions (thick dashed lines) of the central and eastern United States (NCNTRL, Northeast, SCNTRL, and Southeast). The numbers in parentheses correspond to the number of soundings available for each region. Refer to section 2 for a description of the sounding parameters, and section 3b for a discussion of these regional variations.

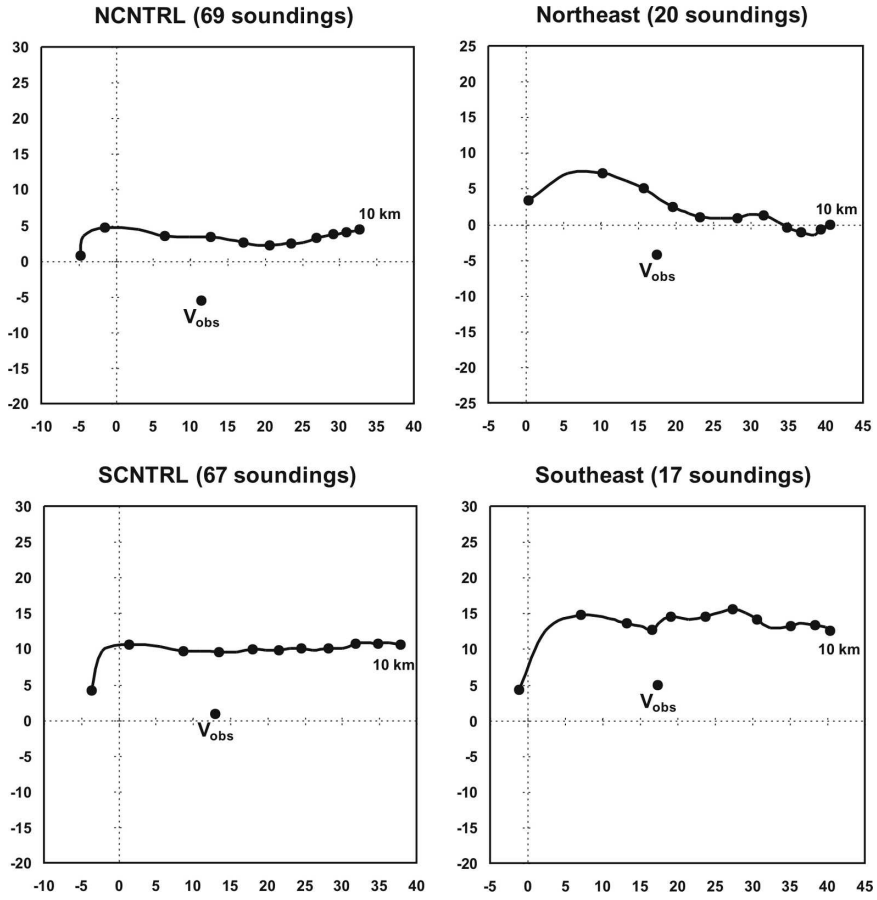

FIG. 10. Composite 0–10-km hodographs and observed storm motions ($m\ s^{-1}$) for the long-lived supercell events for each of four regions of the central and eastern United States. The numbers in parentheses correspond to the number of soundings available for each region. Otherwise the same as in Fig. 5.

dataset was in good agreement with the predicted supercell motion (i.e., 3.5 $m\ s^{-1}$ mean absolute error) using the shear-relative method of Bunkers et al. (2000), indicating there was nothing "unusual" needed to explain why some storms traveled along boundaries. Although this question will not be solved by the present study, the evidence strongly suggests that when the vertical wind shear profile engenders a supercell motion that is closely aligned with a boundary, the probability of supercells being long lived is enhanced (i.e., Fig. 8). Hopefully, additional observational and modeling studies will help provide quantitative guidance to better answer this question.

b. *Regional variations of the long-lived supercell environments*

The regional breakdown of sounding parameters and forcing strength categories helps explain some of the regional differences in supercell properties noted in Part I. Not surprisingly, PWAT was highest, on average, for the long-lived supercell events across the Southeast when compared with the other three regions, especially the NCNTRL (3.37 versus 2.72 cm; Fig. 9). This translated into lower cloud-base heights (MLLCL = 959 versus 1528 m) and less convective inhibition (MLCIN = 27 versus 49 J kg^{-1}) for the Southeast versus the NCNTRL. Given the increased moisture, lower cloud bases, and less convective inhibition across the Southeast, the result should be an increased coverage of thunderstorms. Therefore, it is understandable why the long-lived supercells were less isolated in the Southeast versus the other regions (and especially the NCNTRL).

In terms of atmospheric forcing for the long-lived events, SF environments were much more common in the Southeast (56%) and Northeast (64%) when compared with the NCNTRL and south-central United States (SCNTRL; 11% and 34%, respectively; Fig. 9).

TABLE 7. A summary of pertinent sounding parameters for the examples presented in section 3c. All times are 0000 UTC.

	OUN; 30 May 2004	BIS; 24 Jun 2002	TFX; 6 Aug 2002
$Bulk_{0–8km}$ (m s^{-1})	30.8	21.5	43.1
SRW_{8km} (m s^{-1})	22.6	6.7	24.8
MLBRN	40	18	7
MLLCL (m)	1272	1167	1258
MLCAPE (J kg^{-1})	2214	2483	719
MLCIN (J kg^{-1})	64	9	127
$SRH_{0–3km}$ (m^2 s^{-2})	256	341	274

The majority of the long-lived supercell events across the Southeast occurred during the cold season when SF environments are expected to be most prevalent. The combination of the SF environments, high PWAT, and relatively low MLCIN in the Southeast can further help to explain the small degree of isolation of supercells in this region, as well as the tendency toward linear convection (50% mixed and 11% linear; Part I).

The MF environments were most common across the NCNTRL and SCNTRL during long-lived supercell events (50%–51%; Fig. 9), and WF environments were of secondary importance across the NCNTRL (38%; Fig. 9). These results agree favorably with Roebber et al.'s (2002) numerical modeling study. Nevertheless, there appears to be various combinations of atmospheric forcing strength and local environmental characteristics that can engender long-lived supercells (evident in the differences between the central and eastern United States).

Overall, the deep-layer shear and upper-level storm-relative winds in the long-lived supercell environments were similar among the four regions (cf. $Bulk_{0–8km}$ and SRW_{8km} in Fig. 9). Most of the differences, though minor, were confined to the 4–8-km layer. Synoptically speaking, west-to-northwest flow in the middle to upper troposphere was most common across the northern United States, while there was a greater tendency for west-to-southwest flow across the southern United States (Figs. 9 and 10). The Southeast had the strongest southerly component out of all four regions (Fig. 10).

Examination of the regional hodographs and sounding parameters provides several clues regarding the regional differences in F2–F5 tornado production by the long-lived supercells. First, the strong 0–1-km shear in the composite hodograph for the Southeast (Fig. 10) is a characteristic feature of hodographs associated with supercells that produce strong and violent tornadoes (Markowski et al. 2003). The composite hodograph for the NCNTRL is generally linear above 1 km, and contains the least amount of bulk shear from the surface to 1 km (Fig. 10). One measure of this shear, $SRH_{0–1km}$,

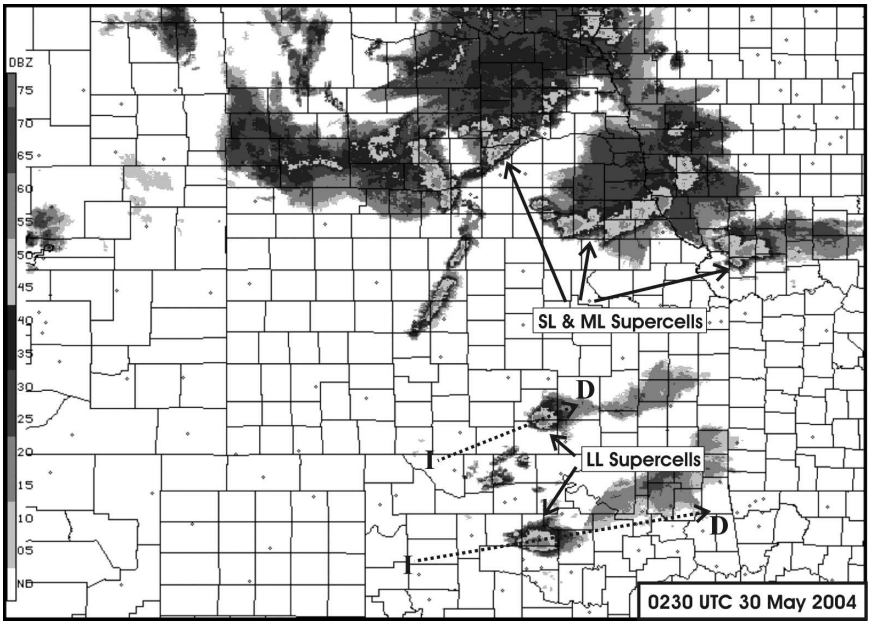

FIG. 11. The 0.5° base reflectivity mosaic image (dBZ) from the WSR-88Ds across the central United States valid at 0230 UTC 30 May 2004. Data are at 2-km resolution. Each "I" represents an initiation point of the long-lived supercell, each "D" represents a point of demise, and each dotted arrow represents a path.

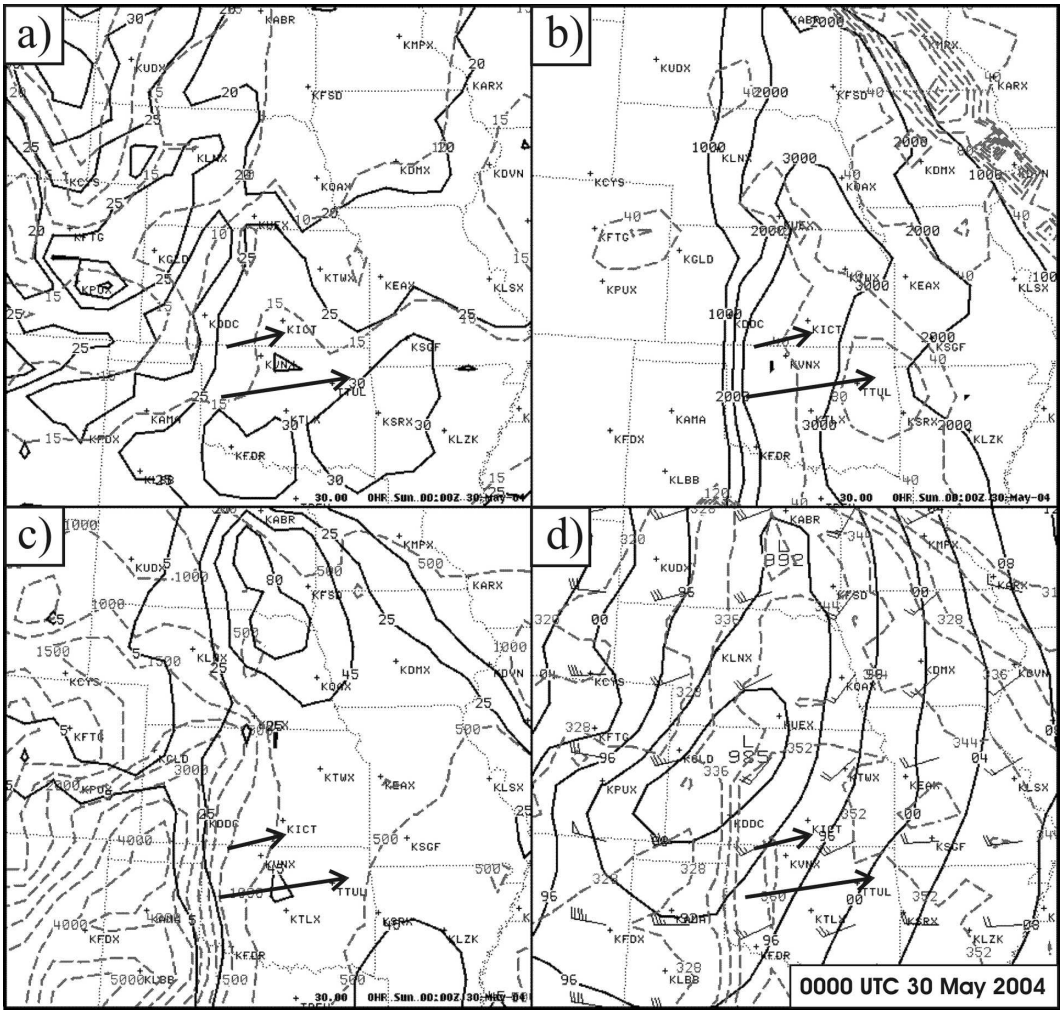

FIG. 12. RUC 0-h analysis valid at 0000 UTC 30 May 2004: (a) $\text{Bulk}_{0\text{–}8\text{km}}$ (solid, $\geq$20 m s^{-1}) and $\text{SRW}_{8\text{km}}$ (dashed; $\geq$10 m s^{-1}), (b) MLCAPE (solid; $\geq$1000 J kg^{-1}) and MLCIN (dashed; absolute value $\geq$ 40 J kg^{-1}), (c) MLBRN (solid; $\geq$5) and MLLCL (dashed; $\leq$5000 m), and (d) mean sea level pressure (solid; 4-hPa contour interval), surface θ_E (dashed; 8-K contour interval), and predicted right-moving supercell motion vectors [m s^{-1} $\times$ 1.94 (kt); Bunkers et al. (2000)]. The boldface arrows indicate the paths of the two long-lived supercells.

was over twice as large in the Southeast versus the NCNTRL (227 versus 102 m^2 s^{-2}; Fig. 9).[5] Second, the MLLCL, which on average is lower in environments where supercells produce F2–F5 tornadoes (Rasmussen and Blanchard 1998; Thompson et al. 2003), was over 600 m lower in the Southeast versus the NCNTRL (959 versus 1528 m; Fig. 9). Third, the MLCIN was strongest over the NCNTRL, possibly reducing the potential for stretching of low-level updrafts and, thus, limiting significant tornadoes (e.g., Davies 2004). Therefore, considering the relatively strong $\text{SRH}_{0\text{–}1\text{km}}$ and low MLLCL heights for long-lived events across the Southeast, combined with only modest convective inhibition, it should be expected that the probability of F2–F5 tornadoes is greater in the Southeast than it is in the NCNTRL. Using these same arguments, further inspection of Figs. 9 and 10 also supports the higher incidence of F2–F5 tornadoes in the Northeast and SCNTRL when compared with the NCNTRL.

A final noteworthy difference in supercell properties among the four regions is that about one-third of the supercells over the central United States evolved into

[5] $\text{SRH}_{0\text{–}1\text{km}}$ averaged 143 m^2 s^{-2} for the entire long-lived supercell dataset, versus 83 and 66 m^2 s^{-2} for the moderate- and short-lived supercell events, respectively (Fig. 6). Recall from Part I the long-lived supercell events produced 2–3 times the number of strong and violent tornadoes per hour when compared to the short-lived events, which is consistent with the higher values of $\text{SRH}_{0\text{–}1\text{km}}$ for the long-lived events (Markowski et al. 2003; Rasmussen 2003).

another form of convection at their demise (e.g., bow echo or squall line; Part I), but only 4% of the events across the eastern United States did so. Given the environmental parameters (Fig. 9), it is possible that the higher MLLCL heights across the central United States contributed to this evolution. These higher cloud bases might have allowed for stronger downdrafts and surface outflow, potentially favoring evolution from supercells to bow echoes or squall lines.

c. Examples and forecasting of supercell longevity

In this section the results from the foregoing discussion are combined with three case studies to illustrate how they may be applied in an operational setting. Pertinent sounding parameters from these three examples are summarized in Table 7.

1) 29 MAY 2004: MULTIPLE SUPERCELL EVENTS IN THE CENTRAL UNITED STATES

The convection on 29 May 2004, which resulted in 87 tornado reports across the central United States, is one of the more obvious examples of supercell longevity. A long-lived supercell event occurred over Oklahoma and far southern Kansas (Fig. 11). The Oklahoma supercell lasted 8.25 h (2300–0715 UTC) while the Kansas supercell lasted 4.5 h (2230–0300 UTC); the supercells reached their demise by way of dissipation. Both of these supercells were quite isolated, associated with a discrete convective mode, and produced F2–F3 tornadoes and hail ≥5.1 cm (≥2 in.). Farther to the north, a mixture of short- and moderate-lived supercells occurred across northeastern Kansas, southeastern Nebraska, and northwestern Missouri (Fig. 11). At times these supercells were accompanied by nearby storms, and the convective mode evolved from discrete to linear throughout the event. Two of the moderate-lived supercells also produced a few significant tornadoes. Short-lived supercells were predominant even farther to the north over northeastern Nebraska and eastern South Dakota (from which only weak tornadoes were reported).

The long-lived supercell event across the SCNTRL occurred in an environment associated with MF (i.e., modest upper-level flow and a surface dryline); the moderate- and short-lived supercell events to the north occurred under SF conditions (i.e., amplified upper-level flow and a surface cold front). A buoyancy axis at the surface was oriented north–south across the central United States with the long-lived supercells occurring in a broad warm sector (Figs. 12b and 12d). $\text{Bulk}_{0\text{–}8\text{km}}$, $\text{SRW}_{8\text{km}}$, MLBRN, and MLLCL were favorable for long-lived supercells across much of Oklahoma and southern Kansas (Figs. 12a, 12c, and 13; also see Table 7), whereas $\text{Bulk}_{0\text{–}8\text{km}}$, $\text{SRW}_{8\text{km}}$, and MLBRN indicated short-lived supercells from northeastern Nebraska through eastern South Dakota (Figs. 12a and 12c). The convective inhibition from the Norman, Oklahoma

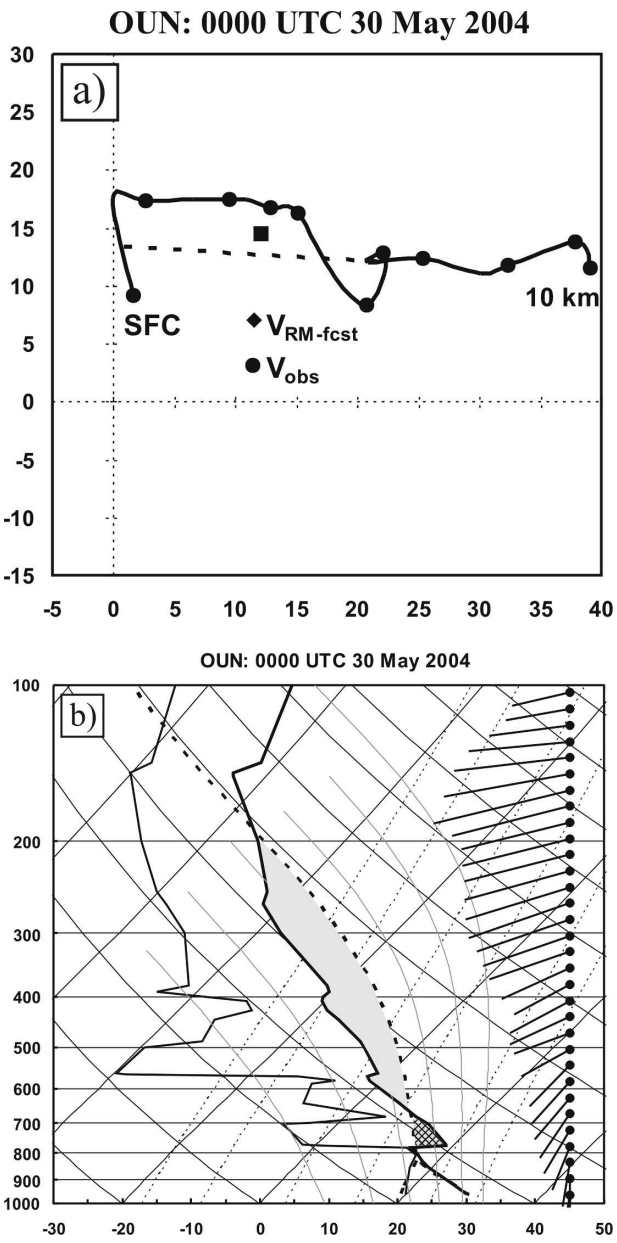

FIG. 13. (a) Observed 0–10-km hodograph (m s^{-1}) for Norman, OK, valid at 0000 UTC 30 May 2004. Here, $\mathbf{V}_{obs}$ is the observed supercell motion, $\mathbf{V}_{RM\text{-}fcst}$ is the predicted right-moving supercell motion (Bunkers et al. 2000), the dashed line represents the 0–0.5- to 5.5–6-km shear vector, and the square is the surface–6-km mean wind. Data are plotted every 500 m, but markers are given only at 1-km intervals. (b) Observed skew *T*–log*p* sounding for Norman valid 0000 UTC 30 May 2004. The ascent path for the 1000-m mean-layer parcel is indicated by the dashed line. MLCAPE is shaded in light gray, and MLCIN is cross-hatched.

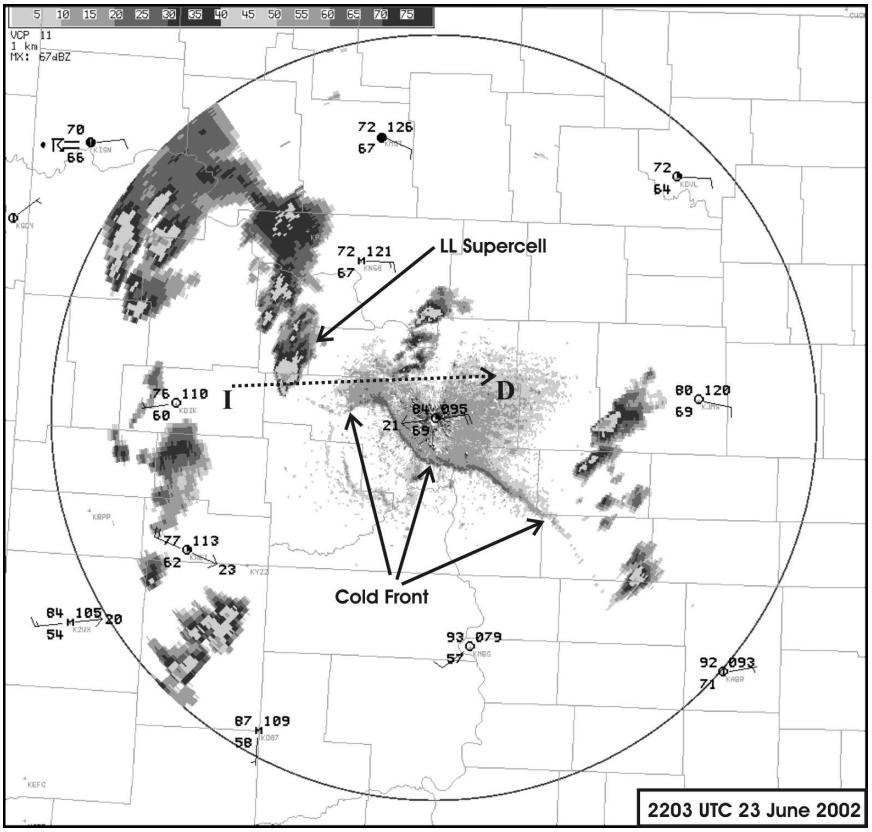

FIG. 14. The 0.5° base reflectivity image (dBZ) from the WSR-88D at Bismarck, ND, valid at 2203 UTC 23 Jun 2002, along with standard surface observations valid at 2200 UTC. The I represents the initiation of the LL supercell, the D represents its demise, and the dotted arrow represents its path. The radius of the range ring is 230 km.

(OUN), sounding also partially explains the isolated nature of the southernmost supercells (Fig. 13b; MLCIN = 64 J kg^{-1}).

In summary, the long-lived supercells fit the prototypical model of being isolated, discrete, and producers of significant tornadoes. All of the parameters were favorable for long-lived supercells in Oklahoma and southern Kansas, and the larger-scale environment also favored the occurrence of long-lived supercells. Convection transitioned to shorter-lived supercells from south to north across the central and northern plains as SF was encountered, the convection became less isolated, and the strength of the deep-layer shear decreased. The SF and nonisolated storms in this northern area led to a relatively rapid upscale growth to linear convection.

2) 23 JUNE 2002: LONG-LIVED SUPERCELL EVENT IN NORTH DAKOTA

The 23 June 2002 long-lived supercell event in central North Dakota was a complex scenario involving the simultaneous occurrence of one isolated long-lived supercell and several other moderate- and short-lived supercells. The isolated long-lived supercell lasted 4.75 h (2100–0145 UTC; Fig. 14), but the average lifespan of all supercells for this event was only around 2.0 h—more characteristic of a short-lived supercell event. The single long-lived supercell generated three severe hail reports and produced one F0 tornado.

The environment across North Dakota was typified by MF [i.e., a 300-hPa isotach maximum around 26 m s^{-1} (50 kt), a modest-amplitude 500-hPa short-wave trough, and a moderate-strength lower-tropospheric baroclinic zone], and initial discrete convection was eventually followed by a transition to a linear convective mode (therefore, this event was classified as mixed). A northwest–southeast-oriented cold front was moving slowly south across central North Dakota, and the long-lived supercell traveled from the warm side to the cold side of the front (Fig. 14), after which it evolved into a bow echo (at point D in Fig. 14). Although the supercell intensified briefly upon intersect-

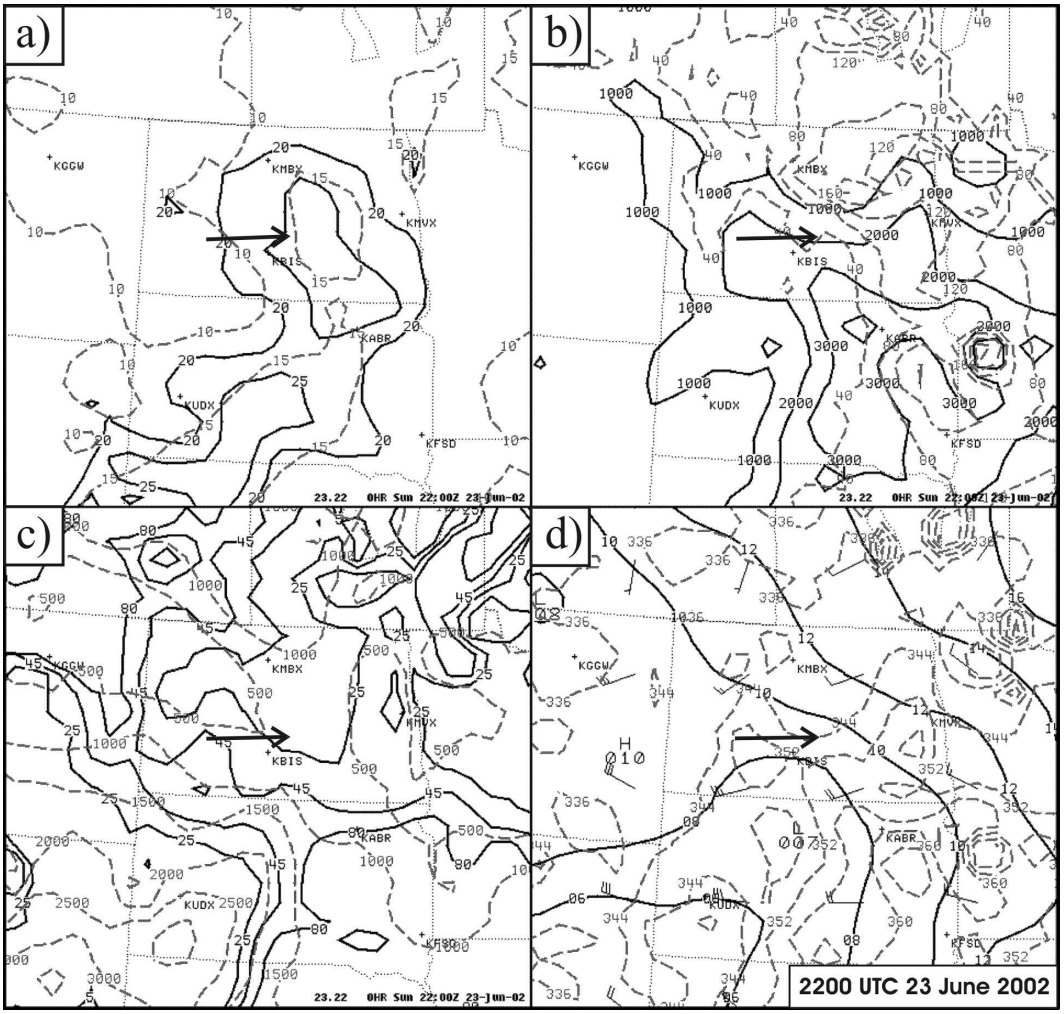

FIG. 15. RUC 0-h analysis valid at 2200 UTC 23 Jun 2002: (a) $\text{Bulk}_{0\text{–}8\text{km}}$ (solid; $\geq$20 m s^{-1}) and $\text{SRW}_{8\text{km}}$ (dashed; $\geq$10 m s^{-1}), (b) MLCAPE (solid; $\geq$1000 J kg^{-1}) and MLCIN (dashed; absolute value $\geq$ 40 J kg^{-1}), (c) MLBRN (solid; $\geq$5) and MLLCL (dashed; $\leq$3000 m), and (d) mean sea level pressure (solid; 2-hPa contour interval), surface θ_E (dashed; 4-K contour interval), and predicted right-moving supercell motion vectors [m s^{-1} $\times$ 1.94 (kt); Bunkers et al. (2000)]. The boldface arrow indicates the path of the long-lived supercell.

ing the boundary, it maintained its due east direction and did not deviate along the boundary. The F0 tornado was produced 85 min after the supercell crossed the boundary, and 39 km toward the cold side (e.g., Markowski et al. 1998).

Sounding parameters provided mixed signals for this case. Values of $\text{Bulk}_{0\text{–}8\text{km}}$ and $\text{SRW}_{8\text{km}}$ were in ranges considered favorable for *short-lived* supercells (cf. Figs. 15a and 16a with Figs. 1 and 2; also see Table 7). However, the MLBRN and MLLCL were in ranges conducive to the occurrence of moderate- and long-lived supercells (cf. Figs. 15c and 16b with Figs. 1, 3, and 4). The track of the long-lived supercell gradually took it toward slightly less buoyant air (Figs. 15b and 15d), but it did stay near the frontal boundary for the first half of its lifetime. It is difficult to say why this one supercell was long lived, and the others were not, but it may have been related to its close proximity to the front; the other supercells did not have as long of a residence time near this boundary. Perhaps if the vertical wind shear profile would have better supported a southeast motion, the supercell would have remained nearer to the front and lived even longer. Rasmussen et al. (2000) also provided documentation of long-, moderate-, and short-lived supercells occurring in close proximity to one another, and a mesoscale boundary appeared to play a key role in the storm evolution.

In summary, this case study shows that long-lived

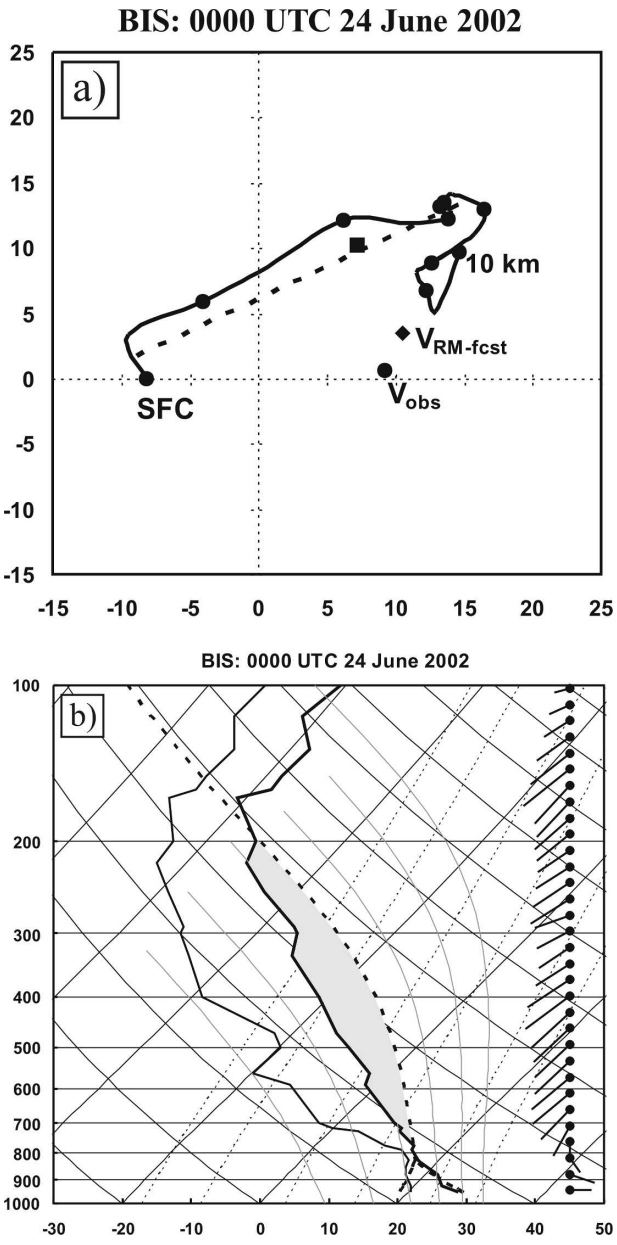

FIG. 16. Same as in Fig. 13 but for Bismarck and valid at 0000 UTC 24 Jun 2002.

supercells can occur when sounding parameters (e.g., shear and storm-relative winds) are not entirely favorable, but the mesoscale environment compensates to locally enhance supercell longevity. The orientation of the cold front could have made the difference between a long-lived versus short-lived supercell event. Moreover, despite suboptimal $\text{Bulk}_{0\text{–}8\text{km}}$ and $\text{SRW}_{8\text{km}}$, very low MLLCL heights likely limited the production of a strong surface outflow, thereby enabling the supercell to be long lived.

3) 5 AUGUST 2002: MODERATE-LIVED SUPERCELL EVENT IN MONTANA

The 5 August 2002 moderate-lived supercell event in Montana is in contrast to the preceding event; several parameters favored long-lived supercells, but only short- to moderate-lived supercells were observed. A radar analysis showed that one short-lived supercell and at least five moderate-lived supercells—some relatively small—occurred in close proximity to each other (four are indicated in Fig. 17). The average lifetime of these six supercells was 2.8 h, and two lasted for 3.75 h. A very brief (<0.75 h) left-moving supercell was also noted. With time, the outflow from the three westernmost supercells (Fig. 17) consolidated, resulting in a small squall line (therefore, this event was classified as mixed mode). The easternmost supercell eventually weakened and became part of a broken line of elevated thunderstorms. This supercell event produced fairly substantial severe weather for the area; three F0 tornadoes were reported and there were 12 severe hail reports.

The environment was considered to be SF because of a highly amplified upper-level trough over the Pacific Northwest, combined with a moderate surface cold front bisecting the area (note the surface observations in Fig. 17). Convective parameters appeared to be strongly conducive to long-lived supercells (Figs. 18 and 19; also see Table 7), with especially strong deep-layer shear and upper-level storm-relative winds in combination with low MLBRN and MLLCL values. However, the westernmost supercells were occurring in somewhat of a "CAPE starved" environment (Fig. 19b) and were traveling well on the cold side of the surface front (note the boldface line in Figs. 18b and 18d). In addition, the easternmost supercell encountered considerable convective inhibition (Fig. 18b), consistent with the capping inversion in the Great Falls, Montana (TFX), sounding (Fig. 19b). Also note that the vertical wind shear was aligned nearly parallel to the surface frontal boundary, which favors a linear convective mode (Dial and Racy 2004).

In summary, this case study shows how examination of the larger-scale environmental forcing, in addition to the local sounding parameters, is important when assessing the potential for long-lived supercells. Instead of being long lived, the supercells evolved into a linear convective mode relatively quickly and thus were short to moderate lived. It appears that both the strong atmospheric forcing and substantial convective inhibition acted in concert to limit the lifetimes of these initially discrete supercells, despite the favorable vertical wind shear profile.

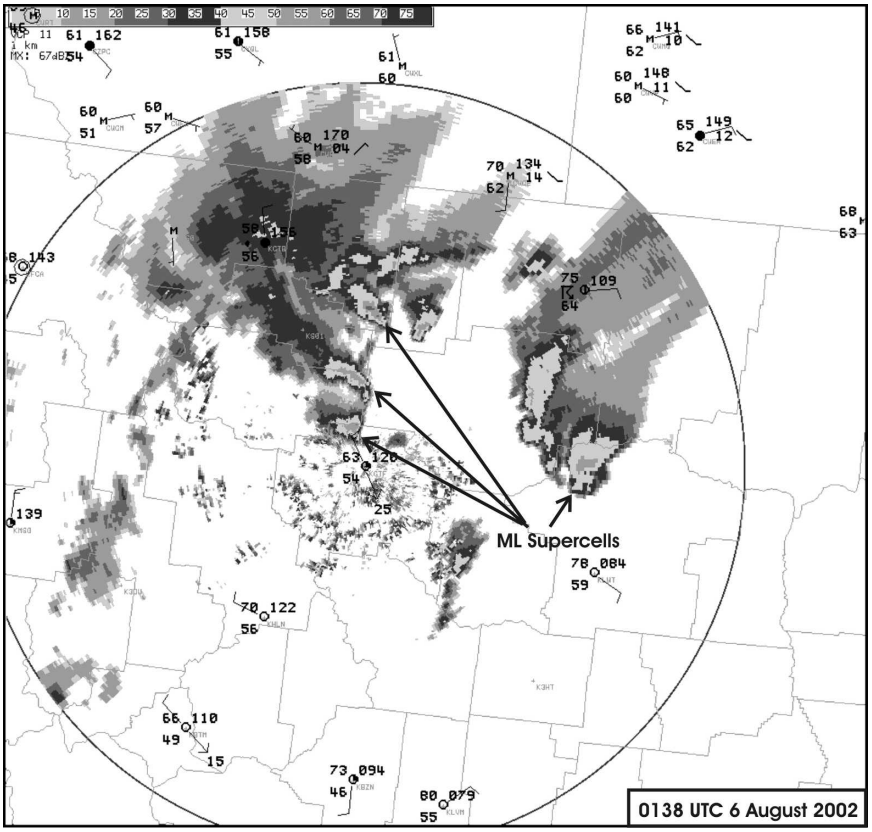

FIG. 17. The 0.5° base reflectivity image (dBZ) from the WSR-88D at Great Falls, MT, valid at 0138 UTC 6 Aug 2002, along with standard surface observations valid at 0200 UTC. The radius of the range ring is 230 km.

4) OTHER CASES

Several additional examples could be used to illustrate the dependence of supercell longevity on supercell motion. For example, the tornado outbreak on 4 May 2003 (NOAA 2005) featured several supercells that were traveling at a large angle (>60°) to a relatively narrow ridge of equivalent potential temperature. Sounding parameters were highly conducive to long-lived supercells within this swath of favorable moisture and buoyancy. And although one long-lived supercell was observed, most supercells were short to moderate lived with an average lifespan of around 3.0 h for the supercells in eastern Kansas, eastern Oklahoma, Missouri, and northern Arkansas. The shortest-lived supercells occurred where the width of the moisture–buoyancy ridge was the smallest.

Last, the fifth-longest-lived supercell in the present dataset (9.5 h), and also the costliest hailstorm on record (Changnon and Burroughs 2003), traveled nearly parallel to a stationary front and within a large region of favorable moisture and buoyancy for its entire lifetime. All of the sounding parameters were favorable for long-lived supercells in this region (i.e., this was one of the more obvious events). Therefore, the local and larger-scale environments appeared to act synergistically in this case to produce an extremely long-lived supercell.

4. Conclusions and summary

The environments of long-lived supercells were compared with those of moderate- and short-lived supercells in an attempt to improve our understanding of these significant storms. Emphasis was placed both on local sounding parameters as well as overviews of the mesoscale to synoptic-scale settings. Moreover, regional variations of these environmental conditions were explored to address some of the questions raised in Part I. Three case studies illustrated how these results may be applied in an operational setting, and they also indicated the complexity that can be associated with these supercell events. Based on the above analyses, the primary conclusions are grouped into three categories.

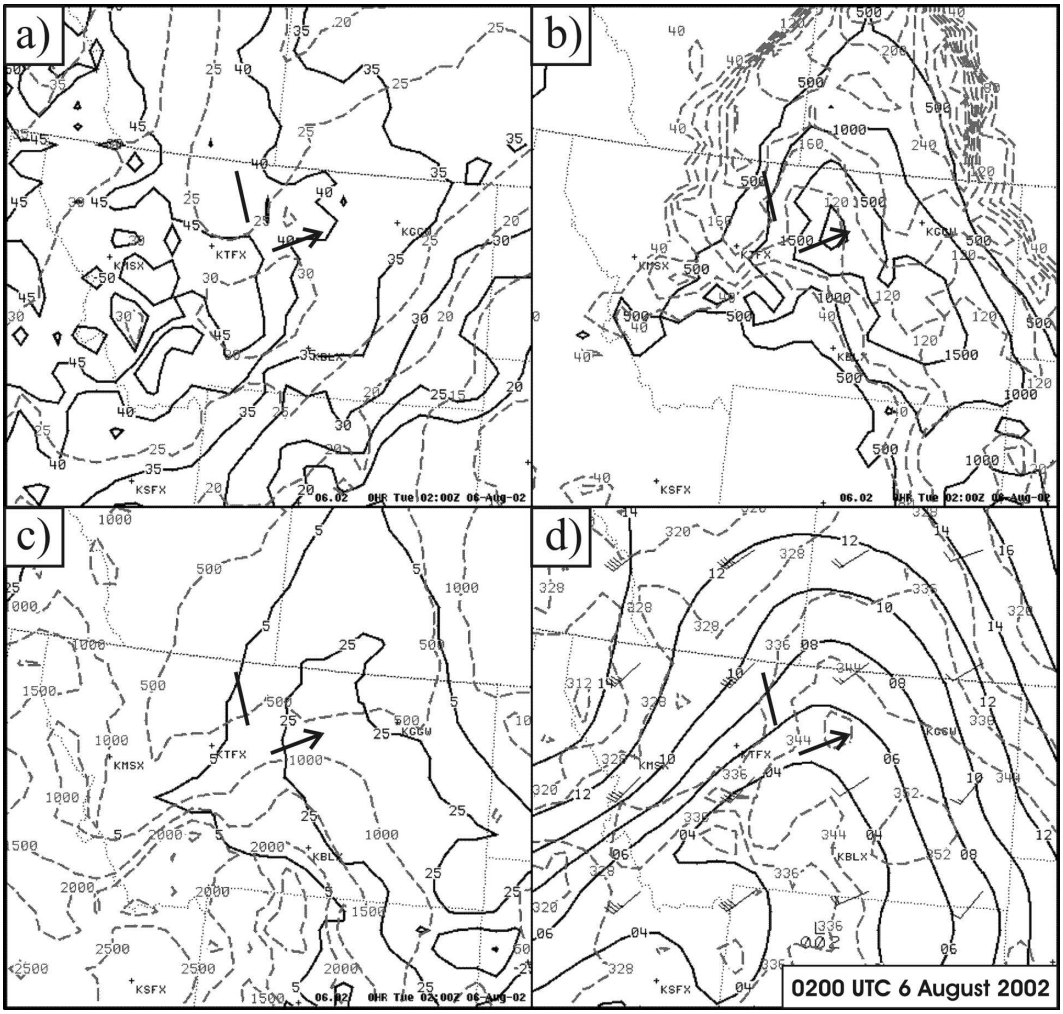

FIG. 18. RUC 0-h analysis valid at 0200 UTC 6 Aug 2002: (a) $\text{Bulk}_{0\text{–}8\text{km}}$ (solid; $\geq$20 m s^{-1}) and $\text{SRW}_{8\text{km}}$ (dashed; $\geq$10 m s^{-1}), (b) MLCAPE (solid; $\geq$500 J kg^{-1}) and MLCIN (dashed; absolute value $\geq$ 40 J kg^{-1}), (c) MLBRN (solid; $\geq$5) and MLLCL (dashed; $\leq$3000 m), and (d) mean sea level pressure (solid; 2-hPa contour interval), surface θ_E (dashed; 8-K contour interval), and predicted right-moving supercell motion vectors [m s^{-1} $\times$ 1.94 (kt); Bunkers et al. (2000)]. The short boldface line indicates the location where three moderate-lived supercells joined to form a line, and the boldface arrow indicates the path of a fourth moderate-lived supercell.

1) The near-storm environment:
   - The 0–8-km bulk wind shear is much stronger in the environments of long-lived supercells when compared with short-lived supercells, leading to stronger 8-km storm-relative winds. These factors support increased updraft strength via enhanced rotation and decreased downdraft strength via curtailed outflow production.
   - A balance between buoyancy and vertical wind shear exists in long-lived supercell environments, such that the MLBRN displays a relatively narrow range mostly from 5 to 45. As the MLBRN increases above 50, buoyancy becomes dominant relative to the shear and such an environment is associated with shorter-lived supercells.
   - Long-lived supercells form in environments that are typically more conducive to producing strong and violent tornadoes (i.e., lower MLLCL heights and stronger $\text{SRH}_{0\text{–}1\text{km}}$) than the environments of short-lived supercells, reinforcing the notion from Part I that there is a connection between supercell longevity and the production of F2–F5 tornadoes.
2) The mesoscale to synoptic-scale environment:
   - Overall, long-lived supercells are most common in MF environments, and short-lived supercells are most common in WF environments; the stronger

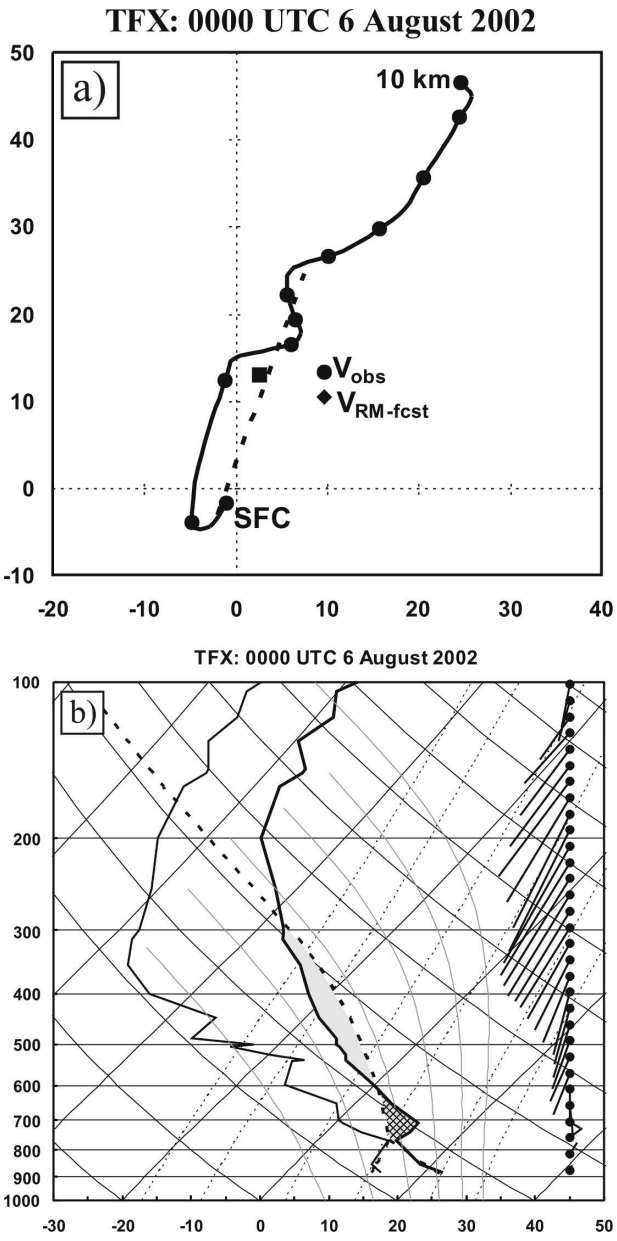

FIG. 19. Same as in Fig. 13 but for Great Falls and valid at 0000 UTC 6 Aug 2002.

the forcing strength, the greater the likelihood of linear and mixed convective modes.

- Supercell motion and longevity are intertwined. Supercell motion somewhat along a boundary or moisture/buoyancy axis, toward increasing moisture and MLCAPE, or within a broad warm sector, is most favorable for long-lived supercells.

3) For the regional comparisons:

- Increased precipitable water, lower cloud-base heights, decreased convective inhibition, and SF environments are associated with the lower frequency of isolated and discrete supercells in the Southeast versus the NCNTRL.
- The MF environments are most common for the long-lived supercell events across the central United States, and SF environments are most common across the eastern United States.
- Cloud-base heights and low-level shear are least favorable for F2–F5 tornadoes in long-lived supercell environments across the NCNTRL—relative to the rest of the central and eastern United States.

The combination of strong deep-layer shear, strong storm-relative winds, small MLBRN, and low MLLCL heights seems to optimize the potential for the longest-lived supercells. First and foremost, strong vertical wind shear both supports updraft rotation and inhibits relatively weak convection, potentially reducing the total number of storms while enhancing the development of the stronger ones (Pastushkov 1975; Weisman and Klemp 1986). Long-lived supercells, therefore, are more isolated and discrete than short-lived supercells. Second, the upper-level storm-relative winds operate to carry hydrometeors away from the updraft, and low MLLCL heights help to reduce subcloud evaporation. Together, these two factors can limit the strength of the downdraft and thus prevent the surface gust front from advancing too far ahead of the updraft. The end result is a strongly rotating storm that has limited interference between the updraft and downdraft and therefore a curtailed outflow production, which enhances the probability for a long lifespan. Finally, the examples revealed that when one of the above parameters is suboptimal, others can partially compensate to aid long-lived supercells (e.g., low MLLCL heights can make up for a lack of deep-layer shear).

Perhaps most noteworthy, supercell motion—with respect to boundaries, moisture/buoyancy axes, and mid- to upper-level forcing mechanisms—has the ability to enhance or limit the longevity of a supercell, which is congruent with the findings of Maddox et al. (1980; their Fig. 1), Wilson and Megenhardt (1997), and Atkins et al. (1999). This relationship may be just as significant as is the near-storm environment in determining supercell longevity. Accordingly, long-lived supercells can exist (be absent) even in environments with weak-to-moderate (strong) shear.

The results of the present study have been synthesized into a simple and highly generalized conceptual model that may be useful as an operational guide when forecasting supercell longevity (Fig. 20). This is not meant to represent all configurations under which long-lived supercells can occur; rather, it should serve as a

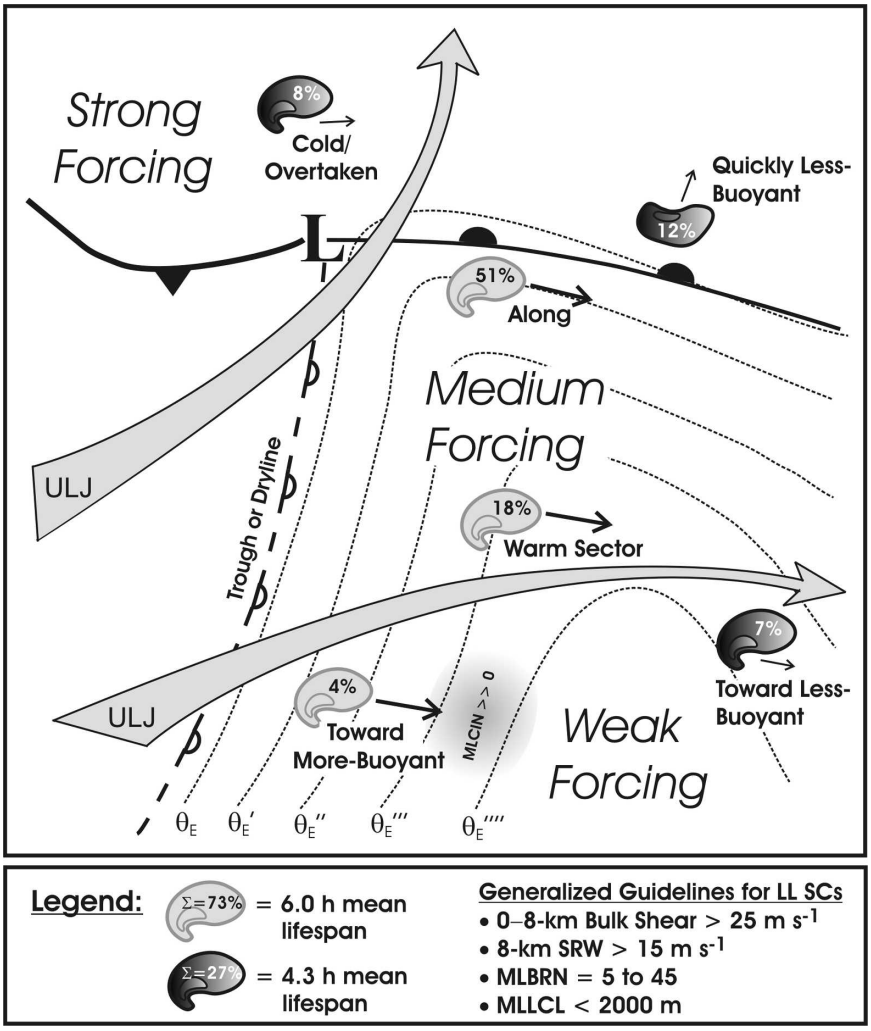

FIG. 20. A highly generalized conceptual model of supercell longevity with guideline values for optimal favorability of long-lived supercells. The synoptic pattern in any specific situation may vary from that shown here; for example, there may not be two jets, the frontal pattern may be different, or the θ_E ridge may have a different orientation. The percentages within the icons represent the relative frequency of long-lived supercells in that particular category as depicted in Fig. 8, and arrows indicate general supercell motions. The mean lifespan for the icons in the legend represents the average duration of all long-lived supercells corresponding to that particular shading. See the end of section 2 for a description of the categories, and refer to sections 3a(2) and 3a(4) for an explanation of the conceptual model.

reminder of the important *processes* (on both the local and larger scales) leading to long-lived supercells. For example, at times the surface equivalent potential temperature (θ_E) ridge may be narrower than shown in Fig. 20, and supercells that travel perpendicular to this may not be long lived. In other circumstances, the buoyancy axis may be oriented north–south with supercell motion right along the axis—a favorable scenario for long-lived supercells. Also note from Fig. 20 that there is typically a spectrum of atmospheric forcing on a given day, supporting a range of convective modes and supercell lifetimes; two upper-level jets need not be present. The left-moving supercell labeled Quickly Less-Buoyant serves as a reminder that elevated supercells can travel toward the cold side of a boundary and still persist for several hours *if* sufficient buoyancy is present above the frontal zone. The "dryline" supercell labeled Toward More-Buoyant demonstrates that some of these potentially long-lived supercells die prematurely as the storm encounters progressively increasing MLCIN (despite moving into more buoyancy). Last, because supercell motion can influence supercell longevity, we recom-

mend overlaying forecast supercell motion vectors on radar/satellite imagery, surface analyses, topographic displays, and even model-derived synoptic fields, which is implied in Fig. 20.

As a final thought, it is tempting to develop a parameter or index of supercell longevity using the results herein as depicted in Fig. 20. However, there are at least two reasons why this might not be prudent. First, a supercell longevity parameter would potentially mask the information gained from looking at the individual parameter fields (e.g., Figs. 12, 15, and 18). Second, a single parameter belies the importance of all other potentially relevant characteristics of the mesoscale to synoptic-scale environment, and could possibly mislead a forecaster into making an incorrect assessment of supercell longevity. Therefore, in order to understand and forecast supercell longevity, we advocate viewing displays similar to those shown in the examples in section 3c. We also note it is imperative to perform a careful subjective analysis of surface and upper-air observations, followed by a careful environmental diagnosis, both of which are vitally important to the forecast process.

In closing, forecasting supercell longevity can be complex at times. But with a basic understanding of the key parameters and environmental conditions, it becomes an achievable goal.

Acknowledgments. We thank (i) the NOAA Central Library, which supplied many of the references pertinent to this study; (ii) Andrew Detwiler, Roger Edwards, Paul Smith, Dennis Todey, and one anonymous reviewer whose comments helped to greatly improve the manuscript; and (iii) David Carpenter, meteorologist-in-charge, at the NWS in Rapid City, South Dakota, for supporting this work.

REFERENCES

Atkins, N. T., M. L. Weisman, and L. J. Wicker, 1999: The influence of preexisting boundaries on supercell evolution. *Mon. Wea. Rev.,* **127,** 2910–2927.

Benjamin, S. G., and Coauthors, 2004: An hourly assimilation–forecast cycle: The RUC. *Mon. Wea. Rev.,* **132,** 495–518.

Bluestein, H. B., and M. L. Weisman, 2000: The interaction of numerically simulated supercells initiated along lines. *Mon. Wea. Rev.,* **128,** 3128–3149.

Brooks, H. E., C. A. Doswell III, and J. Cooper, 1994a: On the environments of tornadic and nontornadic mesocyclones. *Wea. Forecasting,* **9,** 606–618.

——, ——, and R. B. Wilhelmson, 1994b: The role of midtropospheric winds in the evolution and maintenance of low-level mesocyclones. *Mon. Wea. Rev.,* **122,** 126–136.

Browning, K. A., 1977: The structure and mechanisms of hailstorms. *Hail: A Review of Hail Science and Hail Suppression, Meteor. Monogr.*, No. 38, Amer. Meteor. Soc., 1–43.

Bunkers, M. J., B. A. Klimowski, J. W. Zeitler, R. L. Thompson, and M. L. Weisman, 2000: Predicting supercell motion using a new hodograph technique. *Wea. Forecasting,* **15,** 61–79.

——, ——, and ——, 2002: The importance of parcel choice and the measure of vertical wind shear in evaluating the convective environment. Preprints, *21st Conf. on Severe Local Storms*, San Antonio, TX, Amer. Meteor. Soc., 379–382.

——, M. R. Hjelmfelt, and P. L. Smith, 2006: An observational examination of long-lived supercells. Part I: Characteristics, evolution, and demise. *Wea. Forecasting,* **21,** 673–688.

Changnon, S. A., and J. Burroughs, 2003: The tristate hailstorm: The most costly on record. *Mon. Wea. Rev.,* **131,** 1734–1739.

Chisholm, A. J., and J. H. Renick, 1972: The kinematics of multicell and supercell Alberta hailstorms. Alberta Hail Studies, Research Council of Alberta Hail Studies Rep. 72-2, 24–31.

Craven, J. P., R. E. Jewell, and H. E. Brooks, 2002: Comparison between observed convective cloud-base heights and lifting condensation level for two different lifted parcels. *Wea. Forecasting,* **17,** 885–890.

Davies, J. M., 2004: Estimations of CIN and LFC associated with tornadic and nontornadic supercells. *Wea. Forecasting,* **19,** 714–726.

Davies-Jones, R., D. Burgess, and M. Foster, 1990: Test of helicity as a tornado forecast parameter. Preprints, *16th Conf. on Severe Local Storms*, Kananaskis Park, AB, Canada, Amer. Meteor. Soc., 588–592.

Dial, G. L., and J. P. Racy, 2004: Forecasting short term convective mode and evolution for severe storms initiated along synoptic boundaries. Preprints, *22d Conf. on Severe Local Storms*, Hyannis, MA, Amer. Meteor. Soc., CD-ROM, 11A.2.

Doswell, C. A., III, 1987: The distinction between large-scale and mesoscale contribution to severe convection: A case study example. *Wea. Forecasting,* **2,** 3–16.

——, and E. N. Rasmussen, 1994: The effect of neglecting the virtual temperature correction on CAPE calculations. *Wea. Forecasting,* **9,** 625–629.

——, R. Davies-Jones, and D. L. Keller, 1990: On summary measures of skill in rare event forecasting based on contingency tables. *Wea. Forecasting,* **5,** 576–585.

——, D. V. Baker, and C. A. Liles, 2002: Recognition of negative mesoscale factors for severe-weather potential: A case study. *Wea. Forecasting,* **17,** 937–954.

Droegemeier, K. K., S. M. Lazarus, and R. Davies-Jones, 1993: The influence of helicity on numerically simulated convective storms. *Mon. Wea. Rev.,* **121,** 2005–2029.

Elmore, K. L., D. J. Stensrud, and K. C. Crawford, 2002: Ensemble cloud model applications to forecasting thunderstorms. *J. Appl. Meteor.,* **41,** 363–383.

Evans, J. S., and C. A. Doswell III, 2001: Examination of derecho environments using proximity soundings. *Wea. Forecasting,* **16,** 329–342.

Fankhauser, J. C., and C. G. Mohr, 1977: Some correlations between various sounding parameters and hailstorm characteristics in northeast Colorado. Preprints, *10th Conf. on Severe Local Storms*, Omaha, NE, Amer. Meteor. Soc., 218–225.

Gilmore, M. S., and L. J. Wicker, 1998: The influence of midtropospheric dryness on supercell morphology and evolution. *Mon. Wea. Rev.,* **126,** 943–958.

Klimowski, B. A., and M. J. Bunkers, 2002: Comments on "Satellite observations of a severe supercell thunderstorm on 24

July 2000 made during the *GOES-11* science test." *Wea. Forecasting,* **17,** 1111–1117.

LaDue, J. G., 1998: The influence of two cold fronts on storm morphology. Preprints, *19th Conf. on Severe Local Storms,* Minneapolis, MN, Amer. Meteor. Soc., 324–327.

Lemon, L. R., 1980: Severe thunderstorm radar identification techniques and warning criteria. NOAA Tech. Memo. NWS NSSFC-3, 60 pp. [Available from NOAA Central Library, 1315 East–West Highway, Silver Spring, MD 20910.]

Lilly, D. K., 1986: The structure, energetics, and propagation of rotating convective storms. Part II: Helicity and storm stabilization. *J. Atmos. Sci.,* **43,** 126–140.

Maddox, R. A., L. R. Hoxit, and C. F. Chappell, 1980: A study of tornadic thunderstorm interactions with thermal boundaries. *Mon. Wea. Rev.,* **108,** 322–336.

Markowski, P. M., E. N. Rasmussen, and J. M. Straka, 1998: The occurrence of tornadoes in supercells interacting with boundaries during VORTEX-95. *Wea. Forecasting,* **13,** 852–859.

——, J. M. Straka, and E. N. Rasmussen, 2002: Direct surface thermodynamic observations within the rear-flank downdrafts of nontornadic and tornadic supercells. *Mon. Wea. Rev.,* **130,** 1692–1721.

——, C. Hannon, J. Frame, E. Lancaster, A. Pietrycha, R. Edwards, and R. L. Thompson, 2003: Characteristics of vertical wind profiles near supercells obtained from the Rapid Update Cycle. *Wea. Forecasting,* **18,** 1262–1272.

Marwitz, J. D., 1972: The structure and motion of severe hailstorms. Part III: Severely sheared storms. *J. Appl. Meteor.,* **11,** 189–201.

McCaul, E. W., Jr., and C. Cohen, 2002: The impact on simulated storm structure and intensity of variations in the mixed layer and moist layer depths. *Mon. Wea. Rev.,* **130,** 1722–1748.

McNulty, R. P., 1995: Severe and convective weather: A Central Region forecasting challenge. *Wea. Forecasting,* **10,** 187–202.

NOAA, cited 2005: Record tornado outbreaks of May 4–10, 2003. NOAA/NWS Service Assessment. [Available online at http://www.nws.noaa.gov/om/assessments/ pdfs/record-may.pdf.]

Pastushkov, R. S., 1975: The effects of vertical wind shear on the evolution of convective clouds. *Quart. J. Roy. Meteor. Soc.,* **101,** 281–291.

Rasmussen, E. N., 2003: Refined supercell and tornado forecast parameters. *Wea. Forecasting,* **18,** 530–535.

——, and D. O. Blanchard, 1998: A baseline climatology of sounding-derived supercell and tornado forecast parameters. *Wea. Forecasting,* **13,** 1148–1164.

——, and J. M. Straka, 1998: Variations in supercell morphology. Part I: Observations of the role of upper-level storm-relative flow. *Mon. Wea. Rev.,* **126,** 2406–2421.

——, S. Richardson, J. M. Straka, P. M. Markowski, and D. O. Blanchard, 2000: The association of significant tornadoes with a baroclinic boundary on 2 June 1995. *Mon. Wea. Rev.,* **128,** 174–191.

Roebber, P. J., D. M. Schultz, and R. Romero, 2002: Synoptic regulation of the 3 May 1999 tornado outbreak. *Wea. Forecasting,* **17,** 399–429.

Thompson, R. L., R. Edwards, J. A. Hart, K. L. Elmore, and P. Markowski, 2003: Close proximity soundings within supercell environments obtained from the Rapid Update Cycle. *Wea. Forecasting,* **18,** 1243–1261.

——, C. M. Mead, and R. Edwards, 2004: Effective bulk shear in supercell thunderstorm environments. Preprints, *22d Conf. on Severe Local Storms*, Hyannis, MA, Amer. Meteor. Soc., CD-ROM, P1.1.

Turner, D. D., B. M. Lesht, S. A. Clough, J. C. Liljegren, H. E. Revercomb, and D. C. Tobin, 2003: Dry bias and variability in Vaisala RS80-H radiosondes: The ARM experience. *J. Atmos. Oceanic Technol.,* **20,** 117–132.

UCAR, cited 2005: A convective storm matrix: Buoyancy/shear dependencies. Cooperative Program for Operational Meteorology, Education, and Training, Boulder, CO. [Available online at http://meted.ucar.edu/convectn/csmatrix/.]

Weisman, M. L., and J. B. Klemp, 1982: The dependence of numerically simulated convective storms on vertical wind shear and buoyancy. *Mon. Wea. Rev.,* **110,** 504–520.

——, and ——, 1986: Characteristics of isolated convective storms. *Mesoscale Meteorology and Forecasting,* P. S. Ray, Ed., Amer. Meteor. Soc., 331–358.

——, and R. Rotunno, 2000: The use of vertical wind shear versus helicity in interpreting supercell dynamics. *J. Atmos. Sci.,* **57,** 1452–1472.

Wilhelmson, R. B., and J. B. Klemp, 1978: A numerical study of storm splitting that leads to long-lived storms. *J. Atmos. Sci.,* **35,** 1974–1986.

Wilks, D. S., 1995: *Statistical Methods in the Atmospheric Sciences*. Academic Press, 467 pp.

Wilson, J. W., and D. L. Megenhardt, 1997: Thunderstorm initiation, organization, and lifetime associated with Florida boundary layer convergence lines. *Mon. Wea. Rev.,* **125,** 1507–1525.

Zeitler, J. W., and M. J. Bunkers, 2005: Operational forecasting of supercell motion: Review and case studies using multiple datasets. *Natl. Wea. Dig.,* **29,** 81–97.